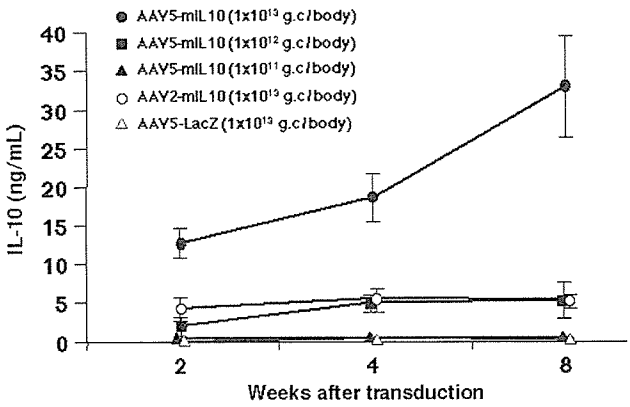

Figure 2 *Serum concentration of IL-10 after transduction of AAV-mIL10 into the anterior tibial muscle of ApoE-deficient mice. ApoE-deficient mice at 8 weeks of age were inoculated with AAV2-mIL10 (1×10^{13} g.c./body), AAV5-mIL10 ($1 \times 10^{11} \sim 1 \times 10^{13}$ g.c./body), or AAV5-LacZ (1×10^{13} g.c./body) by injection into the anterior tibial muscle. At 2, 4, and 8 weeks after injection, the serum IL-10 concentration was measured. Data are means ± s.e.m. ($n = 3$–7).*

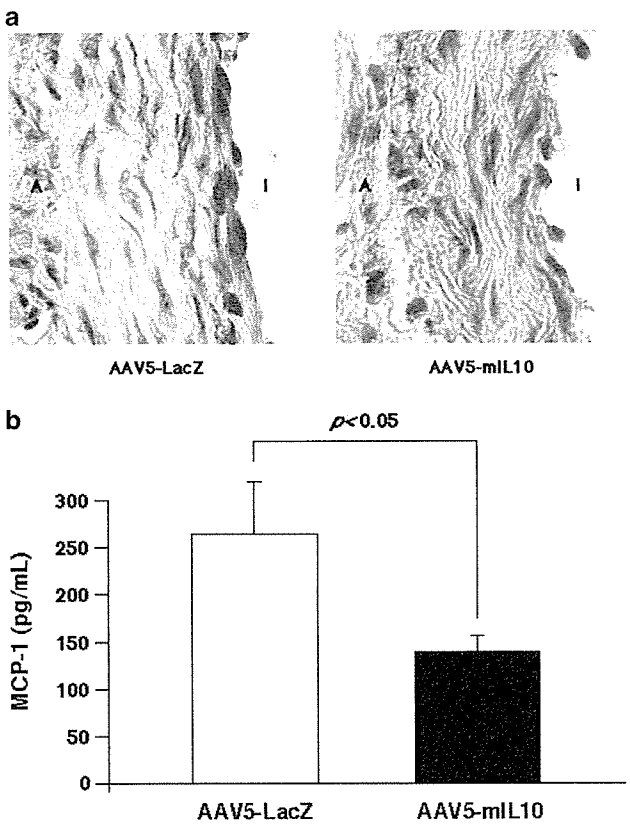

Figure 3 *Systemic and local MCP-1 expression in ApoE-deficient mice. (a) Immunohistochemical staining of the aortic sinus segment in ApoE-deficient mice was performed 4 weeks after inoculation with AAV5-mIL10 (1×10^{12} g.c./body). Enhanced MCP-1 expression was observed in the vascular wall of AAV5-LacZ mice, but was suppressed in AAV5-mIL10-transduced mice. I, intima; A, adventitia. (b) The serum MCP-1 concentration in ApoE-deficient mice was measured 8 weeks after inoculation with AAV5-mIL10 or AAV5-LacZ. Means and s.e.m. for each group are presented as histograms ($n = 6$ for LacZ, $n = 13$ for IL-10).*

red-O-positive areas compared to that of mice transduced with AAV5-LacZ. The systemic overexpression of IL-10 resulted in a 31% reduction in plaque surface area

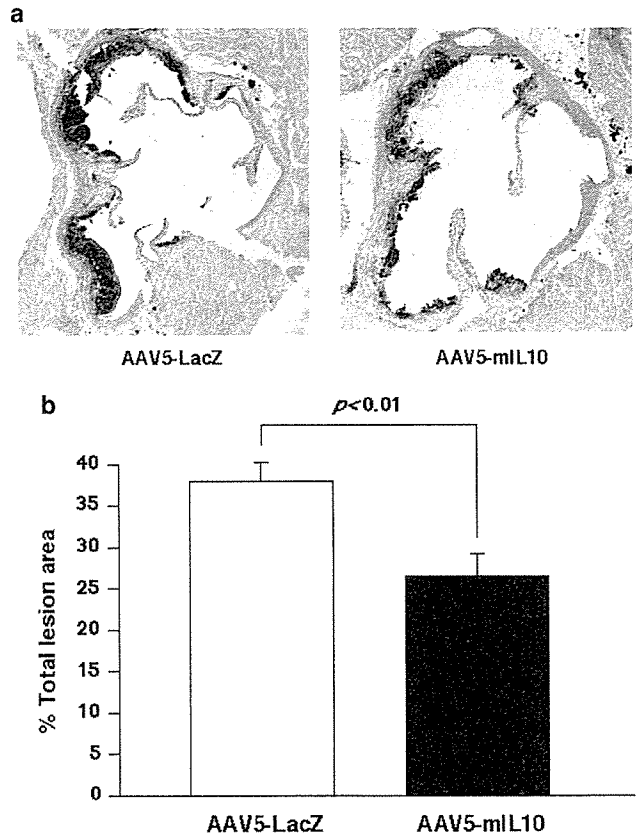

Figure 4 *The inhibitory effect of IL-10 on atherogenesis in ApoE-deficient mice. (a) At 8 weeks after inoculation with AAV5-mIL10 (1×10^{12} g.c./body), the proximal aortas were removed, sectioned, and stained with oil red-O. (b) Oil red-O-positive areas were analyzed in comparison with the total cross-sectional vessel wall area. The average values for five sites from each animal were used for analysis. Means and s.e.m. for each group are presented as histograms ($n = 5$ for LacZ, $n = 9$ for IL-10).*

(AAV5-IL-10, 26.5 ± 1.9% *versus* AAV5-LacZ, 37.7 ± 2.2% of total cross-sectional vessel wall area, $P < 0.01$). Figure 5 shows that serum MCP-1 concentration correlates with the extent of atherosclerotic lesion formation, suggesting that a decrease in MCP-1 expression is related to a decrease in atherosclerotic lesion formation.

Effect of IL-10 on lipids

We investigated the effects of IL-10 expression on the level of serum lipids. Total cholesterol levels were significantly reduced in the AAV5-mIL10-transduced mice (931 ± 432, 1074 ± 419 mg/dl) compared to the AAV5-LacZ-transduced mice (2212 ± 640, 1840 ± 421 mg/dl, 4 weeks and 8 weeks after gene transfer, respectively). Triglyceride level in the AAV5-IL10-transduced mice 8 weeks after gene transfer was also reduced (171.7 ± 67.3 mg/dl) compared to that in the AAV5-LacZ-transduced mice (291.6 ± 172.4 mg/dl, $P < 0.05$).

Nonlinear regression fitting to a sigmoidal dose curve revealed a high correlation between the serum cholesterol level and IL-10 concentration ($r = 0.857$), with an estimated EC_{50} of 5.3 ng/ml (Figure 6a). In addition, the serum cholesterol concentration positively correlated with the atherosclerotic lesion area ($r = 0.728$, $P < 0.01$; Figure 6b). IL-10 gene transfer did not affect body

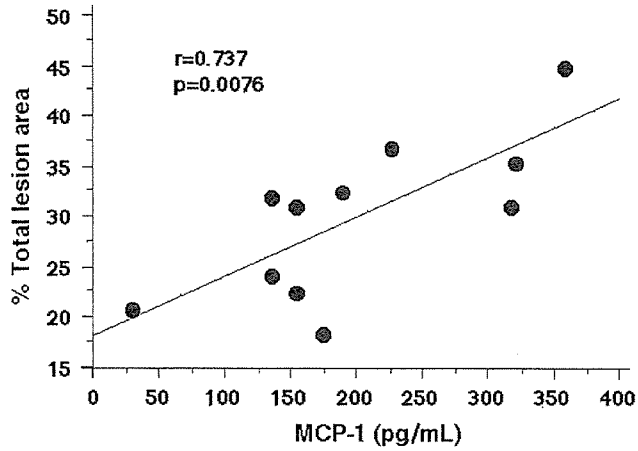

Figure 5 Correlation between serum MCP-1 concentration and extent of atherosclerotic lesion formation. The serum MCP-1 concentration positively correlated with oil red-O-positive surface area in ApoE-deficient mice 8 weeks after inoculation with AAV5-mIL10 ($r=0.737$, $P=0.0076$).

weight, food intake, blood sugar levels, or blood pressure (data not shown).

To assess whether IL-10 causes changes in the lipoprotein profile of apoE-deficient mice, plasma lipoproteins were subjected to agarose gel electrophoresis. No differences in the patterns of lipoprotein expression were observed in AAV5-mIL10-transduced mice and AAV5-LacZ-transduced mice (data not shown).

To further understand the mechanism by which the serum cholesterol level is decreased in AAV5-mIL10-transduced mice, we evaluated cholesterol levels of HepG2 cells, human hepatocytes, incubated in the absence of lipoprotein. As shown in Figure 7, the level of cholesterol in HepG2 cells was significantly decreased by the addition of IL-10 in a dose-dependent manner. The level of intracellular cholesterol was also significantly decreased by the addition of HMG-CoA reductase inhibitor, fluvastatin, to these cells. When HepG2 cells were incubated in the presence of lipoprotein, the level of cholesterol in the conditioned medium was not decreased by the addition of IL-10 (data not shown). These data suggest that IL-10 reduces *de novo* cholesterol synthesis, but does not stimulate cholesterol uptake by hepatocytes. Furthermore, we estimated the effect of IL-10 on the expression of HMG-CoA reductase. Interestingly, IL-10 significantly decreased mRNA levels of HMG-CoA reductase ($P<0.01$), while fluvastatin, enzyme inhibitor, did not alter the expression of the enzyme itself (Figure 8).

Discussion

IL-10, a pleiotropic cytokine produced by Th2-type T cells, B cells, monocytes, and macrophages, has potent anti-inflammatory properties. The main finding of the present study is that AAV vector-mediated IL-10 gene transfer to ApoE-deficient mice following a single intramuscular administration inhibits atherosclerotic lesion formation through the inhibition of MCP-1 expression and the reduction in the level of serum cholesterol.

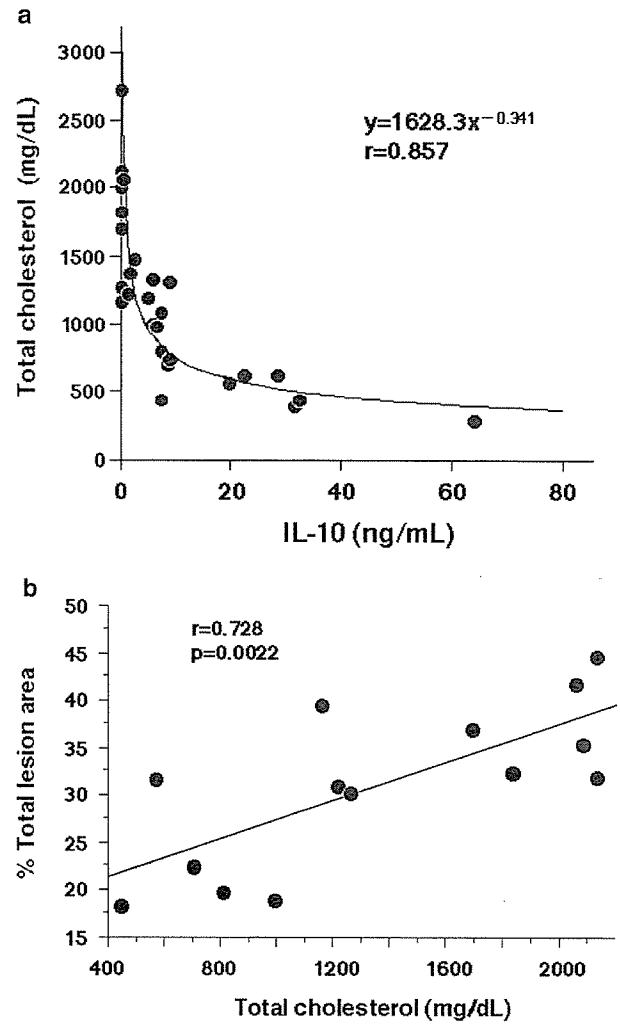

Figure 6 (a) Curve-fitting of the serum cholesterol concentration against the serum IL-10 concentration 8 weeks after inoculation of AAV5-mIL10 yielded a close fit ($r=0.857$) to a dose–response curve ($y=1628.3\times{}^{-0.341}$), with an EC_{50} of 5.3 ng/ml. (b) The serum cholesterol level positively correlated with atherosclerotic lesion surface area 8 weeks after inoculation with AAV5-mIL10 ($r=0.728$, $P=0.0022$).

Differentiated C2C12 cells transduced with AAV2-mIL10 were verified by Western blot analysis and enzyme-linked immunosorbent assay (ELISA) to express IL-10. The biological activity of the secreted IL-10 was also confirmed. Conditioned medium from C2C12 cells transduced with AAV2-mIL10 significantly inhibited the production of IL-6, TNF-α, and MCP-1 by J774 cells in response to LPS treatment. Based on these *in vitro* observations, we used recombinant AAV constructs to evaluate the effects of IL-10 on atherogenesis in ApoE-deficient mice. Intramuscular injection of AAV5-mIL10 into ApoE-deficient mice resulted in long-term systemic IL-10 expression. The serum IL-10 concentration was sustained at levels higher than 398.3 ± 146.6 pg/ml ($n=6$) up to 14 months after gene transfer (1×10^{12} genome copies/body).

Although double-stranded AAV genomes probably remain extrachromosomal in mouse myofibers, their tight association with chromatin allows their persistence and stable expression over periods of several months.[15–17] This particular feature of AAV vectors might be advanta-

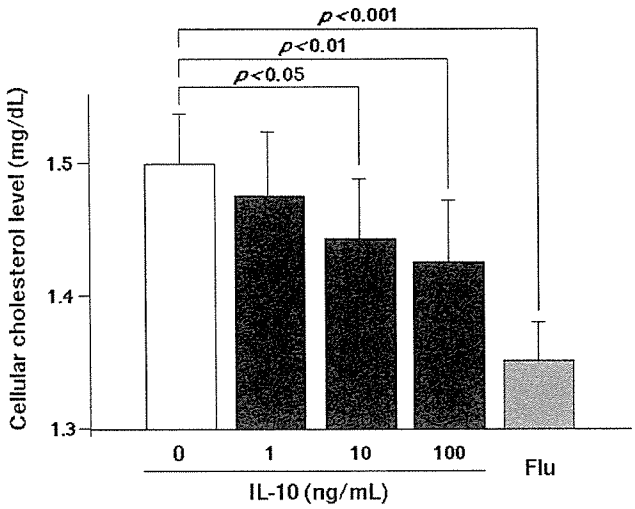

Figure 7 Cellular cholesterol level of HepG2 cells incubated in the absence of LDL cholesterol. Recombinant human IL-10 (1–100 ng/ml) or fluvastatin (10^{-5} mol/l) was added to the culture for 48 h. Data are means ± s.e.m. (n = 4).

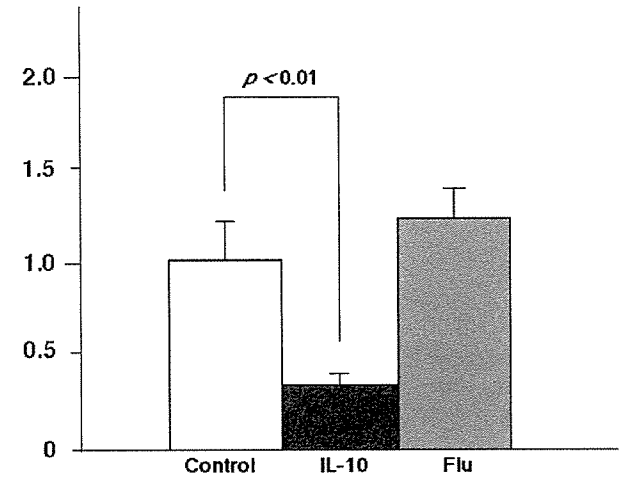

Figure 8 Relative HMG-CoA reductase expression in HepG2 treated with recombinant IL-10 as analyzed by quantitative PCR. The relative expression of the HMG-CoA reductase mRNA was determined as the ratio of the expression in HepG2 treated with IL-10 or fluvastatin to that in HepG2 incubated normally (control). Data are means ± s.e.m. (n = 3–5).

geous in investigating the effects of transgenes on chronic disease processes. Previous reports demonstrated that there was a significant difference in transgene expression by various AAV serotypes transduced into rodent muscle.[18–20] The AAV1 and AAV5 serotypes were shown to produce 100- to 1000-fold higher serum levels of transgene products, as compared to the AAV2. We selected AAV5 for use in *in vivo* experiments, since we also observed that gene transfer with AAV5 promoted a much higher level of expression of IL-10, as compared to AAV2-mediated transfer (Figure 2). However, AAV1 is reported to more efficiently transduce muscle than AAV5. Therefore, we anticipate that the use of AAV1 in future experiments would allow for a minimized vector dosage.

We focused on the effect of IL-10 on *in vivo* MCP-1 expression. MCP-1, one of the most studied members of the C–C family of chemokines, is expressed in several cell types in the arterial wall, including vascular endothelial cells, smooth muscle cells, and monocytes/macrophages, under numerous inflammatory conditions. Therefore, MCP-1 is thought to play an important role in the ongoing recruitment of monocyte–macrophages into developing lesions *in vivo*.[21] Previously, we[22] and others[21,23] reported enhanced MCP-1 expression in experimental and human atherosclerotic lesions. A role for MCP-1 in the initiation of atherogenesis was demonstrated by knockout mice in which the MCP-1 gene itself or its receptor CCR2 was inactivated.[24,25] In our study, we demonstrated that serum MCP-1 concentrations are significantly lower in IL-10-transduced mice than in control mice. In addition, we observed enhanced MCP-1 expression in the vascular wall of ApoE-deficient mice, as reported previously,[26] which was significantly inhibited by IL-10 gene transfer. Moreover, the extent of atherosclerotic lesion formation was significantly decreased in AAV5-mIL10-transduced mice, and positively correlated with serum MCP-1 concentration. These results suggest that the observed antiatherogenic effect of IL-10 is partly mediated by the inhibition of systemic and local MCP-1 expression.

We also investigated the effect of IL-10 on serum cholesterol levels. Nonlinear regression of serum cholesterol levels relative to serum IL-10 levels revealed a close correlation to a dose–effect model with an EC_{50} (5.3 ng/ml). It is well known that high cholesterol levels lead to atherogenesis in both humans and mice. Atherosclerotic lesion surface area also correlated with the serum cholesterol concentration in our study. van Exel *et al*[12] recently found a negative correlation between a low IL-10 production capacity of whole blood and total cholesterol level in humans. They speculated that high levels of IL-10 counteract the effects of TNF-α and IL-6 on lipid metabolism. This clinical observation corresponds well with our observation that the serum IL-10 concentration negatively correlates with the reduction in serum cholesterol.

Pinderski *et al*[8] found that IL-10-transgenic mice showed a decrease in atherosclerotic lesions compared to control mice. However, they found no difference in plasma cholesterol levels between the transgenic and control mice. On the other hand, Von Der Thusen *et al*[13] showed that prolonged hepatic expression of IL-10 could be achieved following intravenous adenovirus-mediated IL-10 gene transfer to LDL receptor-deficient mice. Administration of IL-10 resulted in reductions in atherosclerotic lumen stenosis and of serum cholesterol, although the cholesterol-lowering mechanism was not clarified.

We analyzed the intracellular cholesterol level of HepG2 cells cultured with acetic acid, a cholesterol substrate, in the absence of lipoprotein. This assay can measure *de novo* cholesterol synthesis, but not cholesterol uptake, in these cells. We also used fluvastatin at a dose of 10^{-5} mol/l to inhibit *de novo* cholesterol synthesis almost completely.[27] The results of these experiments suggested that IL-10, like fluvastatin, significantly inhibits the hepatic production of cholesterol. It was reported that TNF-α and IL-1 increase the levels of HMG-CoA reductase mRNA without affecting the levels of LDL receptor mRNA.[28] In other words, the increase in serum cholesterol levels observed after TNF-α and IL-1 administration is caused by an increase in hepatic cholesterol synthesis rather than a decrease in the

clearance of circulating cholesterol. These observations suggest that IL-10 might have direct effects on cholesterol metabolism through the HMG-CoA reductase pathway. We evaluated the expression of HMG-CoA reductase using quantitative PCR. As is expected, IL-10 modulated HMG-CoA reductase expression, whereas fluvastatin did not. These data suggest that the use of IL-10 in combination with statin may improve cholesterol-lowering effects and benefit the patients with atherosclerotic diseases.

Finally, we evaluated whether the downregulation of the MCP-1 was affected by the cholesterol-lowering effects of IL-10 or not. Stepwise regression analysis revealed that not only serum cholesterol but also MCP-1 concentration might be significant independent predictors of atherosclerotic lesion area. Therefore, we speculated that anti-inflammatory effect of IL-10 plays an important role in anti-atherogenic effect as well as its cholesterol-lowering effects.

In summary, AAV5-mediated IL-10-gene transfer into the skeletal muscle could introduce efficient and stable IL-10 expression, resulting in a significant antiatherogenic effects in ApoE-deficient mice. It was suggested that this effect was mediated through the anti-inflammatory and cholesterol-lowering effects of IL-10. These results indicate the presence of complex interactions between inflammation and lipid metabolism, as well as the effectiveness of anticytokine therapy using IL-10 in the treatment of atherosclerotic disease.

Materials and methods

Production of AAV vectors

Two recombinant AAV serotypes, type 2 and type 5, were used in these experiments. AAV2 and AAV5 expressing the *Escherichia coli* β-galactosidase gene under the control of the cytomegalovirus promoter (AAV2-LacZ and AAV5-LacZ) were generated with the proviral plasmids pAAV-LacZ and pAAV5-RNL, respectively. To create AAV2 and AAV5 derivatives expressing murine IL-10 (AAV2-mIL10 and AAV5-mIL10), murine IL-10 cDNA (RIKEN DNA Bank, RDB-1476) was cloned into the *Bam*HI site of pCMV to form pCMVmIL10. The IL-10 expression cassette in pCMVmIL10 was ligated as a *Not*I fragment to *Not*I-digested pAAV-LacZ and pAAV5-RNL to form the proviral plasmids pAAV2-mIL10 and pAAV5-mIL10, respectively.

AAV viral stocks were prepared according to the previously described three-plasmid transfection adenovirus-free protocol.[29] Briefly, 60% confluent 293 cells were cotransfected with the proviral plasmid, an AAV helper plasmid (pHLP19[30] for AAV2 or pAAV5RepCap[31] for AAV5), and the adenoviral helper plasmid pAdeno. The crude viral lysate was purified by two rounds of CsCl two-tier centrifugation.[32] The viral stock was titered by dot-blot hybridization with plasmid standards.

pAAV5-RNL and pAAV5-RepCap (identical to 5RepCapB) were kindly provided by Dr JA Chiorini, and pAAV-LacZ, pHLP19 and pAdeno were obtained from Avigen, Inc. (Alameda, CA, USA).

In vitro IL-10 gene transfer

The C2C12 cells were cultured in six-well plates with 2 ml Dulbecco's minimal essential medium (DMEM) containing 5% horse serum. At 8 days after plating, differentiated C2C12 cells were transduced with AAV2-mIL10 at various vector doses. The expression of IL-10 was detected by Western blot analysis after immunoprecipitation of conditioned medium and cell lysates. IL-10 concentrations were measured by ELISA (R&D Systems). To investigate the biological activities of IL-10, cultured medium from transduced C2C12 cells was added to cultured J774 cells for 30 min (final IL-10 concentration, 10 ng/ml). J774 cells were then treated with 100 ng/ml LPS and incubated for an additional 24 h. The supernatants were harvested and the concentrations of IL-6, TNF-α, and MCP-1 were quantified by ELISA (R&D Systems).

In vivo IL-10 gene transfer

All animal experiments were performed in accordance with the *Jichi Medical School Guide for Laboratory Animals*, 1993. Male ApoE-deficient mice in the C57BL/6J background (a kind gift of Dr N Maeda[33,34]) were fed on a Western-type diet containing 21% fat and 0.15% cholesterol (Harlan Teklad) from 8 weeks of age. Water and food were given *ad libitum*, and the mice were maintained on a 12-h light–dark cycle. At 8 weeks of age, ApoE-deficient mice were injected with AAV2-mIL10 (1×10^{13} genome copies/body), AAV5-mIL10 (1×10^{11}–10^{13} genome copies/body), or AAV5-LacZ (1×10^{13} genome copies/body) as 50 μl in total into two distinct sites of the anterior tibial muscle. The serum concentrations of IL-10 and MCP-1 were measured by ELISA as described above. The serum concentrations of total cholesterol were measured by HDAOS methods (Wako Pure Chemicals).

Morphometric analysis

At 8 weeks after the AAV5-mIL10 or -LacZ inoculation, the ascending aortas were removed after perfusion fixation with 4% paraformaldehyde at physiological pressure, embedded in OCT compound (Tissue-Tek), and frozen in liquid nitrogen. Atherosclerotic lesions in the aortic sinus were examined at five locations separated by 80 μm, with the most proximal site at the point where the aortic valves first appeared, and were stained with oil red-O. To quantify the aortic lesions, each image was digitized and analyzed under a microscope (Olympus) with National Institutes of Health Image software (ver. 1.61). Oil red-O-positive areas were analyzed in comparison with the total cross-sectional vessel wall area. The average value for five locations in each animal was determined.

Immunohistochemical analysis

Arterial sections were prepared from 8-week-old mice transduced with AAV5-IL-10 or AAV5-LacZ at 4 weeks old. These sections were incubated with a primary goat polyclonal antibody against mouse MCP-1 (dilution 1/250, Santa Cruz Biotechnology). Nonspecific IgG was used as a negative control. Sections were incubated with biotinylated anti-mouse secondary antibody and treated with peroxidase-conjugated streptavidin, with 3′, 3′-diaminobenzidine tetrahydrochloride as the enzyme substrate, and counterstained with hematoxylin.

Measurement of cellular cholesterol

HepG2 cells (human hepatocytes) were maintained in a 12-well plate with 1 ml of MEM containing 10% fetal bovine serum, 1% nonessential amino acids (NEAA; ICN), and 1 mmol/l sodium pyruvate at 37°C in a 5% CO_2 incubator for 5 days. The medium was then replaced with 1 ml of MEM containing 10% lipoprotein-deficient serum (LPDS; ICN), 1% NEAA, and 1 mmol/l sodium pyruvate. After 2 days later, the cells were incubated with 1 ml of MEM containing 10% LPDS, 1% NEAA and 1 mmol/l sodium pyruvate, and various concentrations (0–100 ng/ml) of recombinant human IL-10 (PeproTech) or 10^{-5} mol/l fluvastatin (Tanabe) were added to the culture. At 2 days after the treatment, the cells were incubated with 0.5 ml of MEM containing 10% LPDS, 1% NEAA, 1 mmol/l sodium pyruvate, and 2 mmol/l acetic acid for 16 h. The cellular cholesterol level was measured by an enzymatic method using Determiner TC-555 (Kyowa Medics).

mRNA analysis of HMG-CoA reductase

HepG2 cells were incubated with either recombinant human IL-10 (10 ng/ml) or fluvastatin (10^{-5} mol/l) in 10% LPDS medium for 24 h. Total RNA was isolated from the cell culture using an RNeasy Mini kit (QIAGEN) and reverse-transcribed into a single-stranded cDNA using SuperScript Preamplification System (GIBCO BRL). To estimate the expression of HMG-CoA reductase in HepG2, quantitative PCR analysis was conducted by using ABI PRISM 7700 Sequence Detection System (Applied Biosystems). The reaction was performed using the primer pairs specific for the *HMG-CoA reductase* (HMGCR-5′: GGCCCA GTTGTGCGTCTTCC and HMGCR-3′: GTTTGCTGC ATGGGCGTTGTAG) and *GAPDH* (GAPDH-5′: CGCG GGGCTCTCCAGAACATCAT and GAPDH-3′: CCAGCC CCAGCGTCAAAGGTG). Quantitative values were obtained from the threshold cycle (C_t) number that indicated exponential amplification of the PCR product. To normalize each sample, we also quantified the expression of the *GAPDH* gene. The relative target gene expression was also normalized with a calibrator (HepG2 cells without treatment of IL-10 or fluvastatin). The final result, expressed as *N*-fold differences in target gene expression relative to the *GAPDH* gene and the calibrator, was determined by the following formula: $N_{\text{target}} = 2^{\text{correctedΔC}_t\,(\text{GAPDH}-\text{target gene})}$. C_t values of the sample were determined by subtracting the average C_t value of the target gene from the average C_t value of the *GAPDH* gene.

Statistical analysis

Student's *t*-test or ANOVA combined with Scheffe's test was used to compare individual groups, and the Pearson's correlation test was employed to measure the linear association between two variables by using StatView (Abacus Concepts, Inc). Data are presented as means ± s.e.m. A value of $P<0.05$ was considered significant.

Acknowledgements

We thank Dr John A Chiorini for providing pAAV5-RNL and pAAV5-RepCap (identical to 5RepCapB) and Avigen, Inc. (Alameda, CA, USA) for providing pAAV-LacZ, pHLP19, and pAdeno. We also thank Ms. Miyoko Mitsu for her encouragement and technical support. This study was supported in part by Research Grants from the Ministry of Education, Culture, Sports, Science and Technology; the Ministry of Health, Labor and Welfare; the Vehicle Racing Commemorative Foundation; and Mitsui Social Welfare Foundation.

References

1 The Scandinavian Simvastatin Survival Study Group. Randomised trial of cholesterol lowering in 4444 patients with coronary heart disease: the Scandinavian Simvastatin Survival Study (4S). *Lancet* 1994; **344**: 1383–1389.
2 Shepherd J *et al*. Prevention of coronary heart disease with pravastatin in men with hypercholesterolemia. West of Scotland Coronary Prevention Study Group. *N Engl J Med* 1995; **333**: 1301–1307.
3 Chen H, Ikeda U, Shimpo M, Shimada K. Direct effects of statins on cells primarily involved in atherosclerosis. *Hypertens Res* 2000; **23**: 187–192.
4 Feingold KR, Grunfeld C. Role of cytokines in inducing hyperlipidemia. *Diabetes* 1992; **41** (Suppl 2): 97–101.
5 Fiorentino DF, Bond MW, Mosmann TR. Two types of mouse T helper cell. IV. Th2 clones secrete a factor that inhibits cytokine production by Th1 clones. *J Exp Med* 1989; **170**: 2081–2095.
6 Uyemura K *et al*. Cross-regulatory roles of interleukin (IL)-12 and IL-10 in atherosclerosis. *J Clin Invest* 1996; **97**: 2130–2138.
7 Mallat Z *et al*. Expression of interleukin-10 in advanced human atherosclerotic plaques: relation to inducible nitric oxide synthase expression and cell death. *Arterioscler Thromb Vasc Biol* 1999; **19**: 611–616.
8 Pinderski Oslund LJ *et al*. Interleukin-10 blocks atherosclerotic events *in vitro* and *in vivo*. *Arterioscler Thromb Vasc Biol* 1999; **19**: 2847–2853.
9 Mallat Z *et al*. Protective role of interleukin-10 in atherosclerosis. *Circ Res* 1999; **85**: e17–e24.
10 Smith DA *et al*. Serum levels of the antiinflammatory cytokine interleukin-10 are decreased in patients with unstable angina. *Circulation* 2001; **104**: 746–749.
11 Anguera I *et al*. Elevation of serum levels of the anti-inflammatory cytokine interleukin-10 and decreased risk of coronary events in patients with unstable angina. *Am Heart J* 2002; **144**: 811–817.
12 van Exel E *et al*. Low production capacity of interleukin-10 associates with the metabolic syndrome and type 2 diabetes: the Leiden 85-Plus study. *Diabetes* 2002; **51**: 1088–1092.
13 Von Der Thusen JH *et al*. Attenuation of atherogenesis by systemic and local adenovirus-mediated gene transfer of interleukin-10 in LDLr−/− mice. *FASEB J* 2001; **15**: 2730–2732.
14 Kessler PD *et al*. Gene delivery to skeletal muscle results in sustained expression and systemic delivery of a therapeutic protein. *Proc Natl Acad Sci USA* 1996; **93**: 14082–14087.
15 Duan D *et al*. Circular intermediates of recombinant adeno-associated virus have defined structural characteristics responsible for long-term episomal persistence in muscle tissue. *J Virol* 1998; **72**: 8568–8577.
16 Bohl D *et al*. Improvement of erythropoiesis in beta-thalassemic mice by continuous erythropoietin delivery from muscle. *Blood* 2000; **95**: 2793–2798.
17 Shimpo M *et al*. AAV-mediated VEGF gene transfer into skeletal muscle stimulates angiogenesis and improves blood flow in a rat hindlimb ischemia model. *Cardiovasc Res* 2002; **53**: 993–1001.

18 Chao H *et al.* Several log increase in therapeutic transgene delivery by distinct adeno-associated viral serotype vectors. *Mol Ther* 2000; **2**: 619–623.
19 Duan D *et al.* Enhancement of muscle gene delivery with pseudotyped adeno-associated virus type 5 correlates with myoblast differentiation. *J Virol* 2001; **75**: 7662–7671.
20 Rabinowitz JE *et al.* Cross-packaging of a single adeno-associated virus (AAV) type 2 vector genome into multiple AAV serotypes enables transduction with broad specificity. *J Virol* 2002; **76**: 791–801.
21 Yla-Herttuala S *et al.* Expression of monocyte chemoattractant protein 1 in macrophage-rich areas of human and rabbit atherosclerotic lesions. *Proc Natl Acad Sci USA* 1991; **88**: 5252–5256.
22 Seino Y *et al.* Expression of monocyte chemoattractant protein-1 in vascular tissue. *Cytokine* 1995; **7**: 575–579.
23 Nelken NA, Coughlin SR, Gordon D, Wilcox JN. Monocyte chemoattractant protein-1 in human atheromatous plaques. *J Clin Invest* 1991; **88**: 1121–1127.
24 Gu L *et al.* Absence of monocyte chemoattractant protein-1 reduces atherosclerosis in low density lipoprotein receptor-deficient mice. *Mol Cell* 1998; **2**: 275–281.
25 Boring L, Gosling J, Cleary M, Charo IF. Decreased lesion formation in CCR2−/− mice reveals a role for chemokines in the initiation of atherosclerosis. *Nature* 1998; **394**: 894–897.
26 Rayner K, Van Eersel S, Groot PH, Reape TJ. Localisation of mRNA for JE/MCP-1 and its receptor CCR2 in atherosclerotic lesions of the ApoE knockout mouse. *J Vasc Res* 2000; **37**: 93–102.
27 Mascaro C *et al.* Sterol regulatory element binding protein-mediated effect of fluvastatin on cytosolic 3-hydroxy-3-methylglutaryl-coenzyme A synthase transcription. *Arch Biochem Biophys* 2000; **374**: 286–292.
28 Hardardottir I *et al.* Effects of TNF, IL-1, and the combination of both cytokines on cholesterol metabolism in Syrian hamsters. *Lymphokine Cytokine Res* 1994; **13**: 161–166.
29 Matsushita T *et al.* Adeno-associated virus vectors can be efficiently produced without helper virus. *Gene Therapy* 1998; **5**: 938–945.
30 Okada T *et al.* Development and characterization of an antisense-mediated prepackaging cell line for adeno-associated virus vector production. *Biochem Biophys Res Commun* 2001; **288**: 62–68.
31 Chiorini JA, Kim F, Yang L, Kotin RM. Cloning and characterization of adeno-associated virus type 5. *J Virol* 1999; **73**: 1309–1319.
32 Okada T *et al.* Adeno-associated viral vector-mediated gene therapy of ischemia-induced neuronal death. *Methods Enzymol* 2002; **346**: 378–393.
33 Zhang SH, Reddick RL, Piedrahita JA, Maeda N. Spontaneous hypercholesterolemia and arterial lesions in mice lacking apolipoprotein E. *Science* 1992; **258**: 468–471.
34 Ishibashi S *et al.* The two-receptor model of lipoprotein clearance: tests of the hypothesis in "knockout" mice lacking the low density lipoprotein receptor, apolipoprotein E, or both proteins. *Proc Natl Acad Sci USA* 1994; **91**: 4431–4435.

doi:10.1016/j.ymthe.2004.06.146

ARTICLE

High-Level *in Vivo* Gene Marking after Gene-Modified Autologous Hematopoietic Stem Cell Transplantation without Marrow Conditioning in Nonhuman Primates

Kyoji Ueda,[1,2] Yutaka Hanazono,[1,*] Hiroaki Shibata,[1,3] Naohide Ageyama,[3] Yasuji Ueda,[4] Satoko Ogata,[1,4] Toshiaki Tabata,[4] Takeyuki Nagashima,[4] Masaaki Takatoku,[6] Akihiko Kume,[1] Susumu Ikehara,[5] Masafumi Taniwaki,[2] Keiji Terao,[3] Mamoru Hasegawa,[4] and Keiya Ozawa[1,6,*]

[1] *Center for Molecular Medicine and* [6] *Division of Hematology, Department of Medicine, Jichi Medical School, Tochigi 329-0498, Japan*
[3] *Tsukuba Primate Center, National Institute of Infectious Diseases, Ibaraki 305-0843, Japan*
[4] *DNAVEC Corporation, Ibaraki 305-0856, Japan*
[5] *First Department of Pathology, Kansai Medical University, Osaka 570-8506, Japan*
[2] *Division of Hematology and Oncology, Department of Medicine, Kyoto Prefectural University of Medicine, Kyoto 602-8566, Japan*

**To whom correspondence and reprint requests should be addressed at the Center for Molecular Medicine, Jichi Medical School, 3311-1 Yakushiji, Minamikawachi, Tochigi 329-0498, Japan. Fax: +81-285-44-5205. E-mail: hanazono@jichi.ac.jp.*

Available online 15 July 2004

The successful engraftment of genetically modified hematopoietic stem cells (HSCs) without toxic conditioning is a desired goal for HSC gene therapy. To this end, we have examined the combination of intrabone marrow transplantation (iBMT) and *in vivo* expansion by a selective amplifier gene (SAG) in a nonhuman primate model. The SAG is a chimeric gene consisting of the erythropoietin (EPO) receptor gene (as a molecular switch) and c-Mpl gene (as a signal generator). Cynomolgus CD34$^+$ cells were retrovirally transduced with or without SAG and returned into the femur and humerus following irrigation with saline without prior conditioning. After iBMT without SAG, 2–30% of colony-forming cells were gene marked over 1 year. The marking levels in the peripheral blood, however, remained low (<0.1%). These results indicate that transplanted cells can engraft without conditioning after iBMT, but *in vivo* expansion is limited. On the other hand, after iBMT with SAG, the peripheral marking levels increased more than 20-fold (up to 8–9%) in response to EPO even at 1 year posttransplant. The increase was EPO-dependent, multilineage, polyclonal, and repeatable. Our results suggest that the combination of iBMT and SAG allows efficient *in vivo* gene transduction without marrow conditioning.

Key Words: gene therapy, hematopoietic stem cell, intrabone marrow transplantation, nonconditioning, *in vivo* expansion, selective amplifier gene, nonhuman primate

INTRODUCTION

The ability to expand selectively cells containing potentially therapeutic genes *in vivo* would represent an important tool for the clinical application of hematopoietic stem cell (HSC)-based gene transfer. This would circumvent low gene transfer efficiency into HSCs, which is one of the current limitations of this promising technology. Furthermore, the ability to expand genetically modified cells *in vivo* would circumvent another major problem of HSC gene therapy; myeloablative conditioning is necessary unless gene-modified cells have clear growth advantage [1]. Current myeloablative conditioning regimens are associated with high systemic toxicity and potential damage to marrow stroma, possibly resulting in impaired engraftment [2]. With the *in vivo* selection method using a drug-resistance gene, engraftment of transduced cells at low levels may allow successful expansion to clinically relevant levels even without marrow conditioning, although the administration of cytotoxic agents is required for the selection [3]. It has recently been reported that bone marrow cells can efficiently engraft mice without marrow conditioning when implanted directly into the

1525-0016/$30.00

doi:10.1016/j.ymthe.2004.06.146

bone marrow cavity (intrabone marrow transplantation, iBMT) [4,5]. Using the iBMT method, human cord blood cells are also able to engraft efficiently in bone marrow of sublethally irradiated immunodeficient mice [6–8]. Although the iBMT method has been successful in mice, the efficacy in primates remains to be examined.

.We have previously developed a selective amplifier gene (SAG) consisting of a chimeric gene encoding the granulocyte colony-stimulating factor (G-CSF) receptor (as a growth-signal generator) and the hormone-binding domain of the steroid receptor (as a molecular switch) [9]. Hematopoietic cells genetically engineered to express this SAG can be expanded in a steroid-dependent manner *in vitro* and *in vivo* in mice and nonhuman primates [10,11]. Here we have examined such expansion in the setting of nonhuman primate iBMT without marrow conditioning using a new SAG encoding the erythropoietin (EPO) receptor (as a molecular switch) and thrombopoietin receptor (c-Mpl; as a signal generator) [12].

RESULTS

Engraftment after iBMT

First, we examined whether gene-marked CD34$^+$ cells engraft after iBMT using two cynomolgus macaques. Cynomolgus CD34$^+$ cells were transduced with the nonexpression retroviral vector PLI (which contains untranslated sequence) [13]. The transduction results are summarized in Table 1. We injected the transduced CD34$^+$ cells directly into the bone marrow cavity of four proximal limb bones (the femurs and humeri) after gently irrigating the cavity with saline (Fig. 1). This transplant procedure was safely performed without pulmonary embolism or infection of bone marrow. Conditioning treatment such as irradiation was not conducted prior to transplantation. In addition, we returned the transduced CD34$^+$ cells into two monkeys by the conventional transplantation method without prior conditioning.

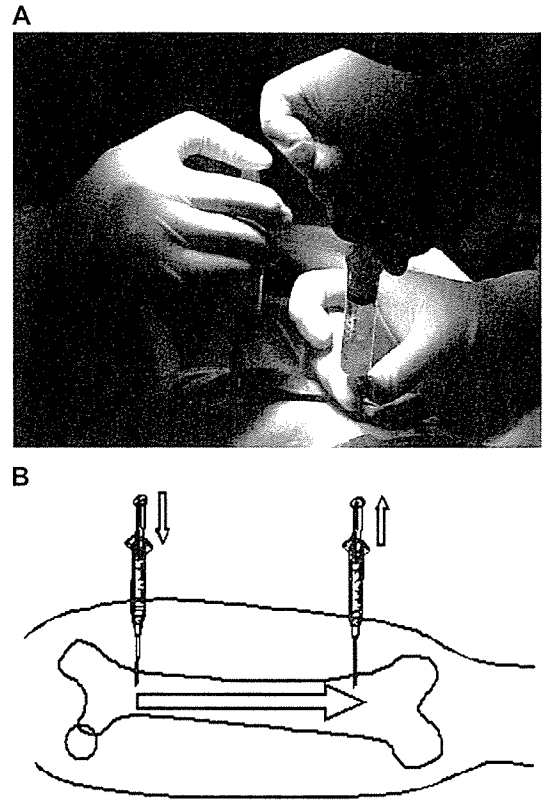

FIG. 1. The iBMT method. We inserted needles at both ends of limb bones (femurs and humeri) and irrigated the bone marrow cavity gently with saline without inflicting extra pressure (A, photo; B, schematic diagram). Gene-modified CD34$^+$ cells were then injected directly into the bone marrow through the needle on one side.

After iBMT, we plated cells from the nonimplanted iliac marrow in methylcellulose medium. We examined the resulting colonies (colony-forming units, CFU) for the provirus by PCR (Fig. 2A and 2B). Two to 30% of colonies (overall 14.2% (74/522)) were positive for the

TABLE 1: *Ex vivo* transduction

Animal	Target cell source	Vector	No. of infused CD34$^+$ cells/kg	Fraction of provirus-positive CFUs in infused CD34$^+$ cells
		Intrabone marrow transplantation		
IB3048	Bone marrow	PLI	4.5×10^7	34/46 (73.9%)
IB3053	Peripheral blood	PLI	8.1×10^6	49/78 (62.8%)
S9042	Peripheral blood	SAG	2.6×10^7	20/35 (57.1%)
S3047	Peripheral blood	SAG	8.1×10^6	11/21 (52.4%)
D8058	Peripheral blood	SAG	7.8×10^5	11/43 (25.6%)
		PLI	5.7×10^5	9/42 (21.4%)
		Intravenous transplantation		
V0065	Peripheral blood	PLI	1.2×10^7	3/45 (6.7%)
V1007	Peripheral blood	PLI	1.5×10^6	14/41 (34.1%)

PLI, nonexpression vector; SAG, selective amplifier gene vector.

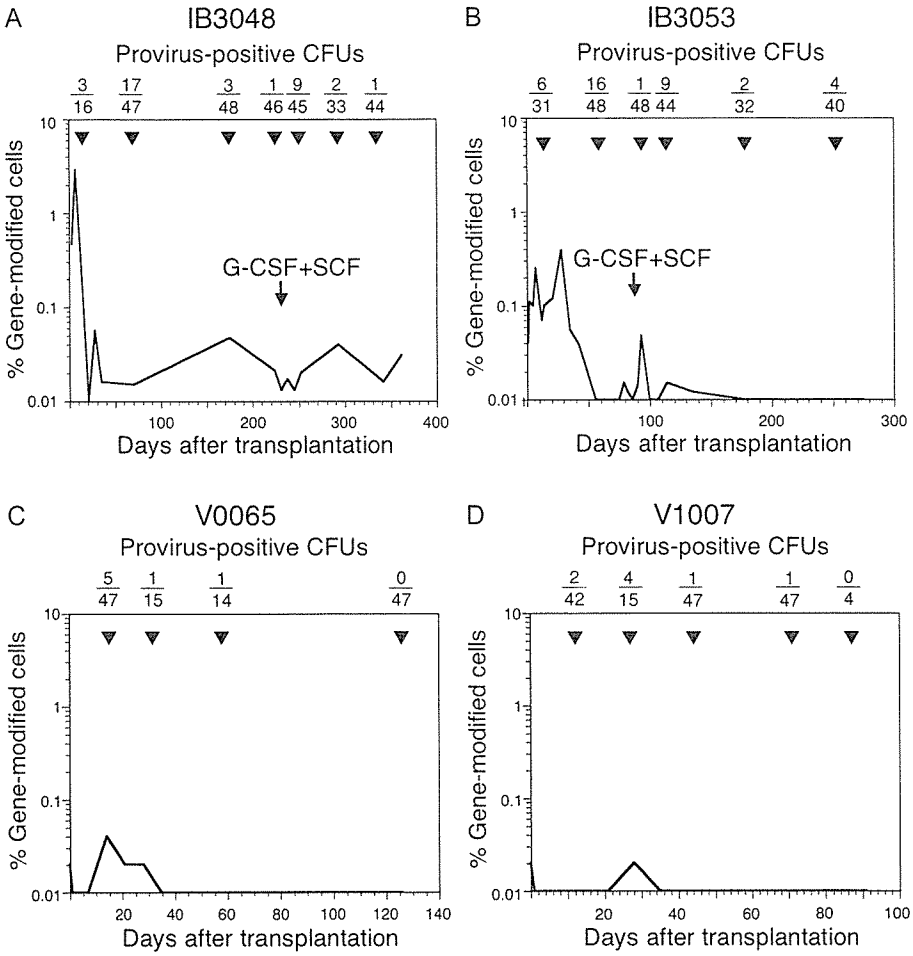

FIG. 2. *In vivo* marking after iBMT and intravenous transplantation without marrow conditioning. $CD34^+$ cells were transduced with nonexpression retroviral vector PLI and returned by iBMT (A, IB3048, and B, IB3053) or by intravenous transplantation (C, V0065, and D, V1007) without conditioning. The upper row shows ratios of provirus-positive CFUs to β-actin-positive CFUs taken from the nonimplanted marrow at time points indicated by arrows. Overall number of provirus-positive CFUs versus overall number of β-actin-positive CFUs was 74/522 (14.2%) for iBMT (A and B) and 15/274 (5.5%) for the intravenous transplantation (C and D). The lower diagram shows percentages of gene-modified cells in the peripheral blood as assessed by quantitative PCR.

provirus and this high marking level persisted for over 1 year posttransplantation. On the other hand, after the conventional intravenous transplantation, generally fewer CFU contained the provirus (overall 5.5% (15/274)) in the bone marrow (Fig. 2C and 2D). Interestingly, the provirus in CFU from the nonimplanted marrow was detectable within 2 weeks after iBMT. Thus, transplanted cells relocated from an implanted bone to another at early time points. A similarly early translocation posttransplantation has also been reported in mouse syngeneic iBMT and human-mouse xeno-iBMT models [4,6–8]. We also examined peripheral blood cells for the provirus by quantitative PCR (Fig. 2A and 2B). The marking levels were, however, very low (<0.1%) in the peripheral blood.

Taken together, these results suggest that transplanted cells can engraft nonconditioned recipients after iBMT but their contribution to the peripheral blood is minimal compared to myeloablated recipients. The cells stay at a resting state in bone marrow without proliferation. In an attempt to proliferate and mobilize iBMT-engrafted resting progenitor cells, we administered G-CSF and stem cell factor (SCF) for 5 consecutive days [14]; however, no obvious increase in the vector-containing cells was observed in the peripheral blood (Fig. 2A and 2B).

EPO-dependent expansion with SAG

We constructed a retroviral vector expressing an SAG that is a chimeric gene of the human EPO receptor gene (extra-plus transmembrane region as a molecular switch) and the human c-Mpl gene (cytoplasmic region as a signal generator) [12]. Cells genetically engineered to express this SAG will proliferate in an EPO-dependent manner. We transduced cynomolgus $CD34^+$ cells with the SAG retroviral vector and introduced them into nonconditioned autologous recipients by iBMT (Table 1). *In vivo* results after transplantation are summarized in Table 2.

In one animal (Fig. 3A), EPO administration triggered a striking elevation in marking levels (7.4% at day 105 posttransplantation) in the peripheral blood. The level of marking in the periphery stayed high for the duration of EPO administration. After cessation of EPO, the level fell to <0.1%. Resumption of EPO administration produced a

doi:10.1016/j.ymthe.2004.06.146

TABLE 2: *In vivo* expansion with SAG after iBMT

	EPO treatment			Marked leukocytes (%)[a]	
Animal	Treatment course	Period (days posttransplant)	Dosage	Basal marking before treatment	Peak marking after treatment (day posttransplant)
S9042	1	1–40	200 IU/kg once daily	NA	7.36% (day 105)
		41–100	200 IU/kg twice daily	NA	7.36% (day 105)
	2	132–210	200 IU/kg twice daily	0.02%	7.72% (day 188)
	3	246–367	200 IU/kg twice daily	0.41%	8.90% (day 348)
S3047	1	75–134	200 IU/kg once daily	0.01%	0.23% (day 145)
		135–166	200 IU/kg twice daily	0.01%	0.23% (day 145)
	2	210–289	200 IU/kg twice daily	0.02%	0.00% (day 289)
D8058	1	1–86	200 IU/kg twice daily	NA	2.30% (day 14)

[a] As assessed by quantitative PCR (see Materials and Methods). NA, not applicable.

similar elevation in the marking levels. The third EPO administration again resulted in the increased marking levels to 8.9% at day 348 posttransplantation. EPO administration was associated with a mild increase in hematocrit (up to 63.5%), which was manageable by occasional phlebotomy. No other adverse effects were observed.

In another animal (Fig. 3B), the SAG-transduced cells increased following transplantation even without exogenous EPO administration. The increase may have been due to increased endogenous EPO elevation resulting from anemia present in the second animal. Overall marking fell with resolution of the anemia. Following resolution, EPO was administered, resulting in an increase in marking levels by more than 20-fold. Marking levels declined to the basal level after discontinuation of EPO. A second attempt to increase marking levels failed, with clearance of SAG-positive cells from the periphery within a month after the second administration, most likely due to cellular immune responses to the xenogeneic SAG (see below).

Multilineage and Polyclonal Expansion

In situ PCR for the proviral sequence showed many transduced cells in the peripheral blood taken from animal S9042 receiving EPO at day 89 posttransplantation (Fig. 4A). We subjected granulocytes and T and B lymphocytes sorted from the peripheral blood of this animal at day 91 posttransplantation to semiquantitative PCR for the provirus. The provirus-containing fraction in granulocytes was 6% and that in B and T lymphocytes was 2% (Fig. 4B), thus indicating that multilineage expansion had occurred. The persistence of marked, short-lived granulocytes for the long term is also another evidence of the successful engraftment of gene-modified HSCs after iBMT. The integration site analysis using the linear amplification-mediated (LAM) PCR method [15]

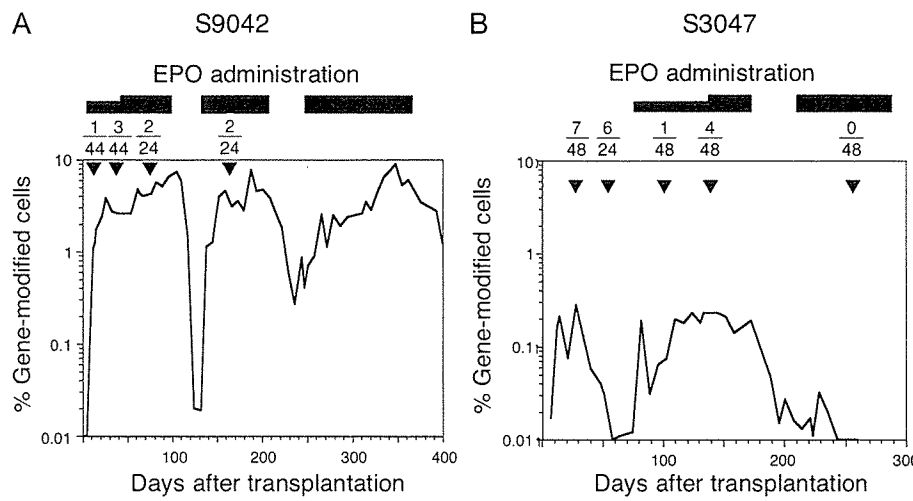

FIG. 3. Expansion of SAG-transduced cells by treatment with EPO after iBMT. $CD34^+$ cells transduced with SAG were returned to each animal by iBMT without conditioning. The animals (A) S9042 and (B) S3047 received EPO at 200 IU/kg once or twice daily (indicated by closed bars). The upper row shows ratios of provirus-positive CFUs to β-actin-positive CFUs taken from the nonimplanted marrow at time points indicated by arrows. The lower diagram shows percentages of gene-modified cells in the peripheral blood as assessed by quantitative PCR.

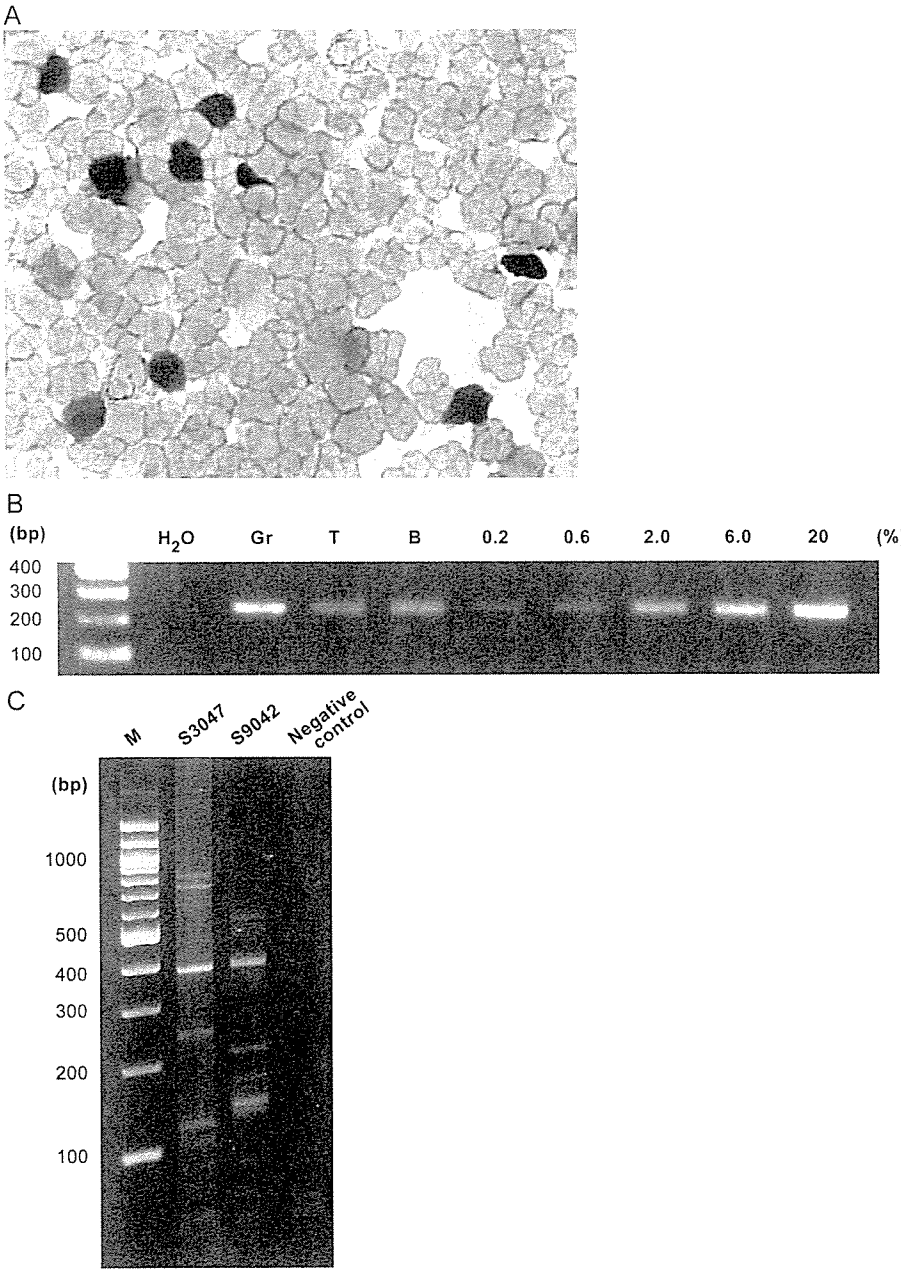

FIG. 4. High-level, multilineage, and polyclonal expansion of gene-modified cells in the peripheral blood after iBMT with SAG in nonconditioned recipients. (A) *In situ* PCR for the provirus. Peripheral blood nucleated cells were collected from animal S9042 receiving EPO at day 89 posttransplantation. Many SAG-transduced cells (stained in black) were detected by *in situ* PCR. (B) Lineage analysis by semiquantitative PCR. DNA from granulocytes (Gr) and T and B lymphocytes sorted from animal S9042 receiving EPO at day 91 posttransplantation was examined for the provirus by semiquantitative PCR. Positive controls corresponding to 0.2, 0.6, 2.0, 6.0, and 20% of transduced cells in peripheral blood were included. (C) Clonal analysis by LAM-PCR. Genomic DNA from peripheral blood of the animals receiving EPO (S9042 at day 90 and S3047 at day 150 posttransplantation) was analyzed by LAM-PCR. Each band indicates different integrants. Negative control was genomic DNA from a naive monkey. M, molecular weight marker.

indicates that the expansion of transduced cells in response to EPO was polyclonal, not mono- or oligoclonal (Fig. 4C).

Dual-Marking Study

We then compared the effects of the SAG vector to a non-SAG vector within, rather than between, individual animals. We harvested cytokine-mobilized peripheral blood $CD34^+$ cells and split them into two equal aliquots. We transduced one aliquot with the SAG vector and the other with the control nonexpression vector (PLI). We mixed both aliquots and returned them by iBMT without marrow conditioning. The animal received EPO from the day after transplantation, and we examined *in vivo* marking levels derived from the two populations by quantitative PCR.

Cells containing the SAG vector increased by 2 logs in the peripheral blood in response to EPO, although cells containing the nonexpression vector remained at low levels (Fig. 5). However, SAG-containing cells were rapidly cleared within 1 month posttransplantation from the periphery and overall SAG-vector marking

doi:10.1016/j.ymthe.2004.06.146

levels became even lower than those from the nonexpression vector-marked fraction. Since cyclosporin A was concomitantly administered to prevent immune responses to human EPO, human EPO concentrations were maintained within an effective range. Thus, it is unlikely that the clearance of xenogeneic human EPO due to immune responses turned off the molecular switch of SAG, resulting in the decrease in SAG-transduced cells.

Immune Responses

The current SAG is a chimeric gene of human origin (the human EPO receptor and human c-Mpl). We collected peripheral lymphocytes from the animal receiving both SAG and nonexpressing PLI (D8058, Fig. 5) at day 169 posttransplantation and examined whether the lymphocytes responded to the xenogeneic SAG *in vitro* (Fig. 6). The response to SAG-transduced target cells was stronger than that to nontransduced target cells (P = 0.05), while the response to PLI-transduced target cells did not differ significantly from that to nontransduced target cells (P = 0.13). The cellular immune response is, therefore, the most likely reason for the clearance of SAG-transduced cells in this animal. This is not novel, but it has been reported that immune responses against transgene products recognized as foreign can indeed be a major obstacle to long-term persistence of gene-modified cells *in vivo* [13,16,17]. In the human clinical setting, however, immune responses should not occur against SAG, because the SAG is made of human genes.

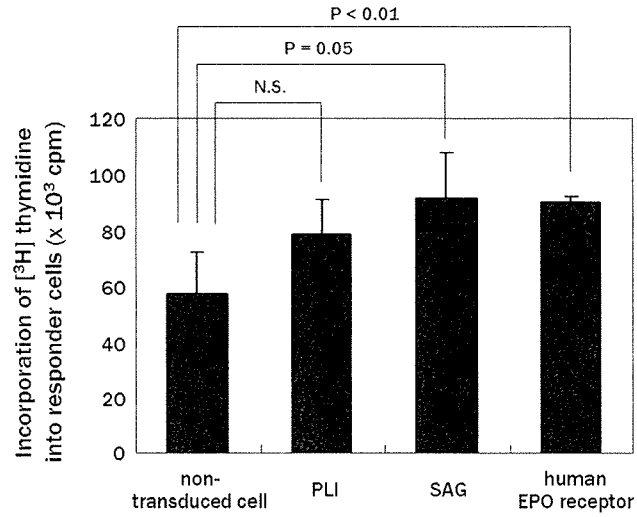

FIG. 6. Positive blastogenic response of lymphocytes to SAG. Peripheral blood mononuclear cells (responder cells) were isolated from monkey D8058 at day 169 posttransplantation (Fig. 5) and cocultured with stimulator cells. The stimulator cells were autologous stromal cells untransduced or transduced retrovirally with PLI, SAG, or human EPO receptor cDNA followed by irradiation with 4000 cGy. After 5 days in culture, the blastogenesis of responder cells was assessed by counting the [^{3}H]thymidine incorporation into responder cells. The averages ± SD of triplicate experiments are shown. N.S., not significant.

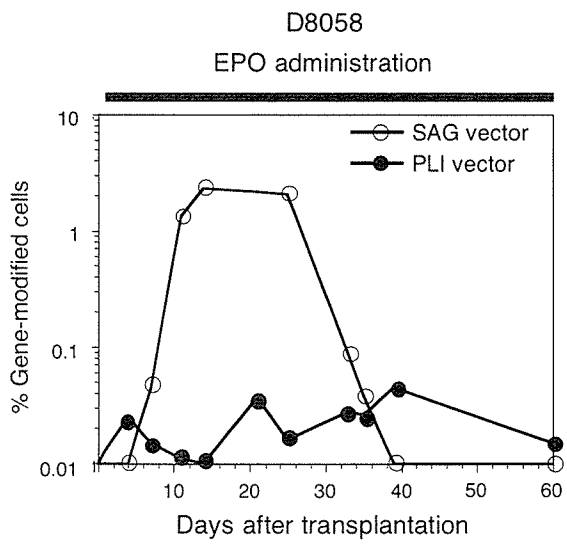

FIG. 5. Dual genetic marking study. CD34$^+$ cells from monkey D8058 were split into two equal aliquots; one aliquot was transduced with SAG vector and the other with nonexpression PLI vector. Both aliquots were together returned to the bone marrow cavity by iBMT without conditioning. EPO (200 IU/kg, twice daily) was administered from the day after transplantation (indicated by a closed bar).

Discussion

Previous papers documented that, without marrow conditioning, very low levels (much less than 0.1%) of cells were marked (or corrected) after CD34$^+$ cell gene therapy of chronic granulomatous disease and Gaucher disease [18,19]. This clinical observation has formed the foundation for the contention that myeloablation (or at least conditioning of reduced intensity) is necessary for successful engraftment of transplanted, genetically modified cells. Our results, however, suggest that nonconditioned iBMT results in much higher gene marking levels (up to 8–9%) through the utilization of an SAG. The physical elimination of endogenous marrow with saline before injection might increase gene marking. In the current study, the marrow of four proximal limb bones (femurs and humeri) was replaced with transplanted cells. If other bones such as the iliac bone (which contains more marrow) are similarly used for iBMT, even higher *in vivo* marking levels may be achieved using an SAG.

Expansion of SAG-transduced cells was seen in three lineages: granulocytes, B lymphocytes, and T lymphocytes. The c-Mpl signal generated by the SAG may work even in lymphocytes. In fact, B lymphocytes were shown to be increased by the activated c-Mpl in a canine trans-

plantation model [20]. The expansion was transient, as is the case with other chimeric genes containing c-Mpl as a signal generator [20], although basal marking levels seemed to increase gradually after repeated EPO administration as shown in Fig. 3A. The method largely results in the selection of transduced cells, not at the level of HSCs, but within the differentiated progeny of transduced HSCs.

In the clinical setting, even if the expansion of gene-modified cells is transient, patients can expect therapeutic effects from EPO administration when used as necessary, such as for infection events in patients with chronic granulomatous disease. EPO is a safe drug and can be administered repeatedly with minimal adverse effects. Polycythemia was the only side effect observed in the present study but was manageable by periodic phlebotomy. Therapeutic effects might also be expected from continuously elevated levels of endogenous EPO, such as in patients with thalassemia. When anemia is ameliorated by the gene therapy and endogenous EPO levels return to physiological levels, then the positive selection system is "automatically" turned off, making this a convenient system in such disorders.

Although this "leave it to patients" system would be convenient, a safety concern may be raised regarding leukemogenesis [21]. The SAG proliferation signal that is persistently turned on *in vivo* by endogenous EPO could trigger a secondary event in addition to possible retroviral insertional mutagenesis, although physiological levels of EPO will not induce a significant proliferative response of SAG [12]. Since a set of EPO-mimetic peptides or a modified EPO such as the erythropoiesis stimulating protein has been developed [22,23], it may be possible to develop an SAG containing a mutant EPO receptor that does not bind to endogenous EPO but binds to such EPO-mimetic peptides or modified EPO.

Materials and Methods

Animals. Cynomolgus monkeys (*Macaca fascicularis*) were housed and handled in accordance with the rules for animal care and management of the Tsukuba Primate Center and the guiding principles for animal experiments using nonhuman primates formulated by the Primate Society of Japan. The animals (2.5–5.6 kg, 3–5 years) were certified free of intestinal parasites and seronegative for simian type-D retrovirus, herpesvirus B, varicella-zoster-like virus, and measles virus. The protocol of experimental procedures was approved by the Animal Welfare and Animal Care Committee of the National Institute of Infectious Diseases (Tokyo, Japan).

Collection of cynomolgus CD34$^+$ cells. Cynomolgus monkeys received recombinant human (rh) SCF (50 μg/kg; Amgen, Thousand Oaks, CA, USA) and rhG-CSF (50 μg/kg; Chugai, Tokyo, Japan) as daily subcutaneous injections for 5 days prior to blood cell collection. Peripheral blood or bone marrow cells were then collected by leukapheresis or by aspiration from iliac bones, respectively. From the harvested cells, the leukocyte cell fraction was obtained after red blood cell lysis with ACK buffer (155 mM NH_4Cl, 10 mM $KHCO_3$, and 0.1 mM EDTA; Wako, Osaka, Japan). Enrichment of CD34$^+$ cells was performed using magnet beads conjugated with anti-human CD34 (clone 561; Dynal, Lake Success, NY, USA), which cross-reacts with cynomolgus CD34 [24]. The purity of CD34$^+$ cells ranged from 90 to 95% as assessed with another anti-human CD34 (clone 563; PharMingen, San Diego, CA, USA) which cross-reacts with cynomolgus CD34 [24]. Mean CFU enrichment was 48-fold as assessed by colony-forming progenitor assays performed before and after enrichment.

Retroviral transduction. We used a retroviral vector expressing SAG (a chimeric gene of the human EPO receptor extra- plus transmembrane region and c-Mpl cytoplasmic region) [12] and PLI nonexpression retroviral vector containing untranslated *neo^R* and β-*gal* sequences [13]. The titers of the viral supernatants used in the present study were both 1×10^6 particles/ml, as assessed by RNA dot blot. CD34$^+$ cells were cultured at a starting concentration of $1-5 \times 10^5$ cells/ml in fresh vector supernatant of PLI or SAG with rhSCF (Amgen), rh thrombopoietin (Kirin, Tokyo, Japan), and rh Flt-3 ligand (Research Diagnostics, Flanders, NJ, USA), each at 100 ng/ml in dishes coated with 20 μg/cm^2 of RetroNectin (Takara, Shiga, Japan). Every 24 h, culture medium was replaced with fresh vector supernatant and cytokines. After 96-h transduction, cells were washed and continued in culture (Dulbecco's modified Eagle's medium (Gibco, Rockville, MD, USA) containing 10% fetal calf serum (Gibco) and 100 ng/ml rhSCF alone) for 2 additional days in the same RetroNectin-coated dishes [25].

Intrabone marrow transplantation. Cynomolgus monkeys were anesthetized. Two needles were inserted into both ends of the femur or humerus [26]. A syringe containing 50 ml of heparin-added saline was connected to one needle and an empty syringe was connected to the other. Normal saline was irrigated gently from one syringe to another through the marrow cavity twice (Fig. 1). Gene-modified cells were suspended in 1 ml of phosphate-buffered saline containing 10% autologous serum and then injected into the marrow cavity and the needle holes were sealed with bone wax (Lukens, Reading, PA, USA). We measured the internal pressure in the marrow cavity during the procedure in some animals and carefully performed saline irrigation and iBMT without inflicting extra pressure on the marrow cavity. No animals suffered from neutropenia, thrombocytopenia, infection, or pulmonary embolism and there was no morbidity. After transplantation, rhEPO (Chugai) was administered to some animals at a dose of 200 IU/kg once or twice daily subcutaneously. Administration of cyclosporin A (Novartis, Basel, Switzerland) to animals was started a week prior to the EPO administration to prevent the development of anti-human EPO antibody [27].

Clonogenic hematopoietic progenitor assays. Cells were plated in a 35-mm petri dish in 1 ml of α-minimum essential medium containing 1.2% methylcellulose (Shin-Etsu Chemicals, Tokyo, Japan) supplemented with 100 ng/ml rh interleukin-3 (PeproTech, Rocky Hill, NJ, USA), 100 ng/ml rh interleukin-11 (PeproTech), 100 ng/ml rhSCF (Biosource, Camarillo, CA, USA), 2 U/ml rhEPO (Roche, Basel, Switzerland), 20% fetal calf serum, 1% bovine serum albumin, 5×10^{-5} M 2-mercaptoethanol (Sigma, St. Louis, MO, USA), and antibiotics (100 U/ml penicillin and 0.1 mg/ml streptomycin). RhEPO was not added to the culture for colony formation from SAG-transduced cells, to avoid excess proliferative response of the transduced cells to EPO. After incubation for 14 days at 37°C with 5% CO_2, colonies containing more than 50 cells were counted using an inverted light microscope. Experiments were conducted in triplicate.

Quantitative PCR. Genomic DNA was extracted using the QIAamp DNA Blood Mini Kit (Qiagen, Chatsworth, CA, USA). DNA (250 ng) was amplified in triplicate with *neo*-specific primers for PLI (5′ -TCCATCATGGATGCAATGCGGC-3′ and 5′ -GATAGAAGGCGATGCGCTGCGAATCG-3′) or with SAG-specific primers (5′ -GACGCTCTCCCTCATCCTCGT-3′ and 5′ -GAGGACTTGGGGAGGATTTCA-3′). Standards consisted of DNA extracted from an SAG- or PLI-producer cell line (which has a known copy number of the proviral sequence) serially diluted with control cynomolgus genomic DNA. Negative controls consisted of DNA extracted from peripheral blood cells of naive monkeys. A β-actin-specific primer set (5′ -

doi:10.1016/j.ymthe.2004.06.146

CCTATCAGAAAGTGGTGGCTGG-3′, 5′-TTGGACAGCAAGAAAGTGAGCTT-3′) was used to certify equal loading of DNA per reaction. Reactions were run using the Qiagen SYBR Green PCR Master Mix (Qiagen) on the ABI Prism 7700 sequence detection system (Applied Biosystems, Foster City, CA, USA) using the following conditions: 50°C for 2 min and 95°C for 15 min, followed by 40 cycles of 94°C for 15 s, 62°C for 30 s, 72°C for 30 s, and 83°C for 15 s. The quantitative PCR was certified each time to yield linear amplifications in the range of the intensity of a positive control series (0.01–100%, correlation coefficient >0.98). For calculating the transduction efficiencies, the C_t value of the vector sequence was normalized based on the C_t value of the internal control β-actin sequence on the same sample as directed in the manufacturer's protocol. Gene marking percentages were calculated given that each provirus-positive cell contains one copy of the vector sequence.

Colony PCR. Well-separated, individual colonies at day 14 were plucked into 50 μl of distilled water, digested with 20 μg/ml proteinase K (Takara) at 55°C for 1 h followed by 99°C for 10 min, and assessed for the SAG or nonexpression PLI vector sequence by nested PCR. The outer primer sets were the same as were used in the quantitative PCR described above. Amplification conditions for the outer PCR were 95°C for 1 min, 54°C for 1 min, and 72°C for 2 min with 20 cycles. The outer PCR products were purified using MicroSpin S-400 HR Columns (Amersham, Piscataway, NJ, USA). The inner primer set for the SAG vector was 5′-CCACCCCTAGCCCTAAATCTTATG-3′ and 5′-GGTGGTTCAGCATCCAATAAGG-3′, and that for the PLI vector was 5′-ATACGCTTGATCCGGCTACCTG-3′ and 5′-GATACCGTAAAGCACGAGGAAG-3′. Amplification conditions for the inner PCR were 95°C for 1 min, 54°C for 1 min, and 72°C for 2 min with 20 cycles. Simultaneous PCR for the β-actin sequence was also performed to certify DNA amplification of the sample in each colony. The primer set for β-actin was the same as was used in the quantitative PCR described above. Amplification conditions for β-actin PCR were 95°C for 1 min, 54°C for 1 min, and 72°C for 2 min with 30 cycles. The final PCR products were separated on 2% agarose gels. The sizes of the products were 206, 483, and 232 bp for SAG, nonexpressing PLI vector, and β-actin sequences, respectively. The transduction efficiency of CFU was calculated by dividing the number of colonies positive for the vector sequence by the number positive for the β-actin sequence. Plucked methylcellulose not containing colonies served as negative controls.

In situ PCR. *In situ* detection of transplanted cell progeny was performed by amplifying the SAG sequence as previously reported [28]. Peripheral blood nucleated cells were spun down to glass slides. The SAG-specific primer sequences were the same as were used for the quantitative PCR described above. The reaction mixture consisted of 420 μM dATP, 420 μM dCTP, 420 μM dGTP, 378 μM dTTP, 42 μM digoxigenin-labeled dUTP (Roche), 0.8 μM each SAG primer, 4.5 mM $MgCl_2$, PCR buffer (Mg^{2+} free), and 4 U Takara *Taq* DNA polymerase (Takara). Slides were covered with the Takara Slide Seal for *in situ* PCR (Takara). PCR was performed using the PTC100 Peltier thermal cycler (MJ Research, Watertown, MA, USA) under the following conditions: 94°C for 1 min and 55°C for 1 min with 15 cycles. The digoxigenin-incorporated DNA fragments were detected using the horseradish peroxidase (HRP)-conjugated rabbit F(ab′) anti-digoxigenin antibody (Dako). Slides were then stained for HRP using the Vector SG Substrate Kit. Finally, slides were counterstained with Kernechtrot dye that stains nucleotides, mounted in glycerol, and examined under a light microscope.

LAM-PCR. The LAM-PCR was performed as previously described [15]. The genomic-proviral junction sequence was preamplified by repeated primer extension using 0.25 pmol of vector-specific, 5′-biotinylated primer LTR1 (5′-AGCTGTTCCATCTGTTCTTGGCCCT-3′) with *Taq* polymerase (2.5 U; Qiagen) from 100 ng of each sample DNA. One hundred cycles of amplification were performed with the addition of fresh *Taq* polymerase (2.5 U) after 50 cycles. Biotinylated extension products were selected with 200 μg of magnetic beads (Dynabeads Kilobase BINDER Kit; Dynal). The samples were incubated with Klenow polymerase (2 U; Roche), dNTPs (300 μM; Pharmacia, Uppsala, Sweden), and a random hexanucleotide mixture (Roche) in a volume of 20 μl for 1 h at 37°C. Samples were washed on the magnetic particle concentrator (Dynal) and incubated with *Tas*I (Fermentas, Hanover, MD, USA) to cut the 5′ long terminal repeat-flanking genomic DNA for 1 h at 65°C. After an additional wash step, 100 pmol of a double-stranded asymmetric linker cassette and T4 DNA ligase (6 U; New England Biolabs, Beverly, MA, USA) was incubated with the beads in a volume of 10 μl at 16°C overnight. Denaturing was performed with 5 μl of 0.1 N NaOH for 10 min at room temperature. Each ligation product was amplified with *Taq* polymerase (5 U; Qiagen), 25 pmol of vector-specific primer LTR2a (5′-AACCTTGATCTGAACTTCTC-3′), and linker cassette primer LC1 (5′-GACCCGGGAGATCTGAATTC-3′) by 35 cycles of PCR (denaturation at 95°C for 60 s, annealing at 60°C for 45 s, and extension at 72°C for 60 s). Of each PCR product, 0.2% served as a template for a second, nested PCR with internal primers LTR3 (5′-TCCATGCCTTGCAAAATGGC-3′) and LC2 (5′-GATCTGAATTCAGTGGCACAG-3′) under identical conditions. Final products were separated on a 2% agarose gel.

Flow-cytometric sorting. We used the FSC/SSC profile (forward and side scatter) to sort granulocytes (purity 95%). Anti-CD3 and anti-CD20 were used to sort T lymphocytes (purity 99%) and B lymphocytes (purity 95%), respectively. Cells were sorted using an EPICS Elite cell sorter equipped with an argon-ion laser (Beckman Coulter, Fullerton, CA, USA). Data acquisition and analysis were performed using the EXPO2 software (Beckman Coulter).

Cellular immune response assay. Peripheral blood mononuclear cells and bone marrow stromal cells were isolated from monkey D8058. The stromal cells were transduced with a retroviral vector carrying the PLI, SAG, or human EPO receptor cDNA. The transduced stromal cells were irradiated with 4000 cGy and used as stimulator cells. Untransduced stromal cells irradiated with 4000 cGy served as a control. The peripheral blood mononuclear cells (responder cells, 2×10^5/well) were cocultured with the stimulator or control cells (5×10^4/well) in 96-well, flat-bottom plates with RPMI 1640 medium (Sigma) containing 10% fetal calf serum and 20 IU/ml rh interleukin-2 (Shionogi, Osaka, Japan). After 5 days in culture, the blastogenesis of responder cells was assessed. Briefly, the cells were labeled with 1 μCi/well of [*methyl*-^{3}H]thymidine (Amersham) for 16 h and harvested with an automated cell harvester (Laboratory Science, Tokyo, Japan) onto glass-fiber filters (Molecular Devices, Sunnyvale, CA, USA). The incorporation of [*methyl*-^{3}H]thymidine into responder cells was quantified in a liquid scintillation counter (Aloka, Tokyo, Japan). All experiments were performed in triplicate.

ACKNOWLEDGMENTS

We are grateful to Aki Takaiwa and Naomi Terao for technical assistance. We thank Cynthia E. Dunbar for help in performing LAM-PCR. We also thank John F. Tisdale for helpful comments on the manuscript. We acknowledge Novartis' supply of cyclosporin A, Amgen's supply of SCF, Ajinomoto's supply of IL-6, Chugai's supply of G-CSF and EPO, and Kirin's supply of thrombopoietin. This study was supported by the Ministry of Health, Labor, and Welfare of Japan and by the Ministry of Education, Culture, Sports, Science, and Technology of Japan.

RECEIVED FOR PUBLICATION MARCH 1, 2004; ACCEPTED JUNE 7, 2004.

REFERENCES

1. Cavazzana-Calvo, M., *et al.* (2000). Gene therapy of human severe combined immunodeficiency (SCID)-X1 disease. *Science* **288:** 669–672.
2. Plett, P. A., Frankovitz, S. M., and Orschell-Traycoff, C. M. (2002). In vivo trafficking, cell cycle activity, and engraftment potential of phenotypically defined primitive hematopoietic cells after transplantation into irradiated or nonirradiated recipients. *Blood* **100:** 3545–3552.
3. Bowman, J. E., Reese, J. S., Lingas, K. T., and Gerson, S. L. (2003). Myeloablation is not required to select and maintain expression of the drug-resistance gene, mutant MGMT, in primary and secondary recipients. *Mol. Ther.* **8:** 42–50.

4. Zhong, J. F., Zhan, Y., Anderson, W. F., and Zhao, Y. (2002). Murine hematopoietic stem cell distribution and proliferation in ablated and nonablated bone marrow transplantation. *Blood* **100:** 3521–3526.
5. Nakamura, K., *et al.* (2004). Enhancement of allogeneic hematopoietic stem cell engraftment and prevention of GVHD by intra-bone marrow transplantation plus donor lymphocyte infusion. *Stem Cells* **22:** 125–134.
6. Wang, J., *et al.* (2003). SCID-repopulating cell activity of human cord blood-derived $CD34^-$ cells assured by intra-bone marrow injection. *Blood* **101:** 2924–2931.
7. Mazurier, F., Doedens, M., Gan, O. I., and Dick, J. E. (2003). Rapid myeloerythroid repopulation after intrafemoral transplantation of NOD-SCID mice reveals a new class of human stem cells. *Nat. Med.* **9:** 959–963.
8. Yahata, T., *et al.* (2003). A highly sensitive strategy for SCID-repopulating cell assay by direct injection of primitive human hematopoietic cells into NOD/SCID mice bone marrow. *Blood* **101:** 2905–2913.
9. Ito, K., *et al.* (1997). Development of a novel selective amplifier gene for controllable expansion of transduced hematopoietic cells. *Blood* **90:** 3884–3892.
10. Kume, A., *et al.* (2003). In vivo expansion of transduced murine hematopoietic cells with a selective amplifier gene. *J. Gene Med.* **5:** 175–181.
11. Hanazono, Y., *et al.* (2002). In vivo selective expansion of gene-modified hematopoietic cells in a nonhuman primate model. *Gene Ther.* **9:** 1055–1064.
12. Nagashima, T., *et al.* (2004). In vivo expansion of gene-modified cells by a novel selective amplifier gene utilizing the erythropoietin receptor as a molecular switch. *J. Gene Med.* **6:** 22–31.
13. Heim, D. A., *et al.* (2000). Introduction of a xenogeneic gene via hematopoietic stem cells leads to specific tolerance in a rhesus monkey model. *Mol. Ther.* **1:** 533–544.
14. Horsfall, M. J., Hui, C. H., To, L. B., Begley, C. G., Basser, R. L., and Simmons, P. J. (2000). Combination of stem cell factor and granulocyte colony-stimulating factor mobilizes the highest number of primitive haemopoietic progenitors as shown by pre-colony-forming unit (pre-CFU) assay. *Br. J. Haematol.* **109:** 751–758.
15. Schmidt, M., *et al.* (2003). Clonality analysis after retroviral-mediated gene transfer to $CD34^+$ cells from the cord blood of ADA-deficient SCID neonates. *Nat. Med.* **9:** 463–468.
16. Riddell, S. R., *et al.* (1996). T-cell mediated rejection of gene-modified HIV-specific cytotoxic T lymphocytes in HIV-infected patients. *Nat. Med.* **2:** 216–223.
17. Rosenzweig, M., *et al.* (2001). Induction of cytotoxic T lymphocyte and antibody responses to enhanced green fluorescent protein following transplantation of transduced CD34(+) hematopoietic cells. *Blood* **97:** 1951–1959.
18. Malech, H. L., *et al.* (1997). Prolonged production of NADPH oxidase-corrected granulocytes after gene therapy of chronic granulomatous disease. *Proc. Natl. Acad. Sci. USA* **94:** 12133–12138.
19. Dunbar, C. E., *et al.* (1998). Retroviral transfer of the glucocerebrosidase gene into CD34+ cells from patients with Gaucher disease: in vivo detection of transduced cells without myeloablation. *Hum. Gene Ther.* **9:** 2629–2640.
20. Neff, T., *et al.* (2002). Pharmacologically regulated in vivo selection in a large animal. *Blood* **100:** 2026–2031.
21. Hacein-Bey-Abina, S., *et al.* (2003). LMO2-associated clonal T cell proliferation in two patients after gene therapy for SCID-X1. *Science* **302:** 415–419.
22. Wrighton, N. C., *et al.* (1996). Small peptides as potent mimetics of the protein hormone erythropoietin. *Science* **273:** 458–464.
23. Macdougall, I. C. (2000). Novel erythropoiesis stimulating protein. *Semin. Nephrol.* **20:** 375–381.
24. Shibata, H., *et al.* (2003). Collection and analysis of hematopoietic progenitor cells from cynomolgus macaques (Macaca fascicularis): assessment of cross-reacting monoclonal antibodies. *Am. J. Primatol.* **61:** 3–12.
25. Takatoku, M., *et al.* (2001). Avoidance of stimulation improves engraftment of cultured and retrovirally transduced hematopoietic cells in primates. *J. Clin. Invest.* **108:** 447–455.
26. Kushida, T., *et al.* (2002). Comparison of bone marrow cells harvested from various bones of cynomolgus monkeys at various ages by perfusion or aspiration methods: a preclinical study for human BMT. *Stem Cells* **20:** 155–162.
27. Schuurman, H. J., *et al.* (2001). Pharmacokinetics of cyclosporine in monkeys after oral and intramuscular administration: relation to efficacy in kidney allografting. *Transplant. Int.* **14:** 320–328.
28. Haase, A. T., Retzel, E. F., and Staskus, K. A. (1990). Amplifications and detection of lentiviral DNA inside cells. *Proc. Natl. Acad. Sci. USA* **87:** 4971–4975.

ELSEVIER

EXPERIMENTAL HEMATOLOGY

Experimental Hematology 32 (2004) 375–381

Ascorbic acid restores sensitivity to imatinib via suppression of Nrf2-dependent gene expression in the imatinib-resistant cell line

Takahisa Tarumoto[a], Tadashi Nagai[a], Ken Ohmine[a], Takuji Miyoshi[a], Makiko Nakamura[a], Takahito Kondo[b], Kenji Mitsugi[c], Syuji Nakano[c], Kazuo Muroi[d], Norio Komatsu[a], and Keiya Ozawa[a]

Divisions of [a]Hematology and [d]Cell Transplantation and Transfusion, Jichi Medical School, Tochigi, Japan; [b]Department of Biochemistry and molecular Biology in Disease, Atomic Bomb Disease Institute, Nagasaki University Graduate School of Medicine, Nagasaki, Japan; [c]First Department of Internal Medicine, Faculty of Medicine, Kyushu University, Fukuoka, Japan

(Received 11 August 2003; revised 1 December 2003; accepted 15 January 2004)

Objective. **Imatinib, a BCR/ABL tyrosine kinase inhibitor, has shown remarkable clinical effects in chronic myelogenous leukemia. However, the leukemia cells become resistant to this drug in most blast crisis cases. The transcription factor Nrf2 regulates the gene expression of a number of detoxifying enzymes such as γ-glutamylcysteine synthetase (γ-GCS), the rate-limiting enzyme in glutathione (GSH) synthesis, via the antioxidant response element (ARE). In this study, we examined the involvement of Nrf2 in the acquisition of resistance to imatinib. Since oxidative stress promotes the translocation of Nrf2 from the cytoplasm to the nucleus, we also examined whether ascorbic acid, a reducing reagent, can overcome the resistance to imatinib by inhibiting Nrf2 activity.**

Results. **Binding of Nrf2 to the ARE of the γ-GCS light subunit (γ-GCSl) gene promoter was much stronger in the imatinib-resistant cell line KCL22/SR than in the parental imatinib-sensitive cell line KCL22. The levels of γ-GCSl mRNA and GSH were higher in KCL22/SR cells, a finding consistent with the observation of an increase in Nrf2-DNA binding. Addition of a GSH monoester to KCL22 cells resulted in an increase in the IC_{50} value of imatinib. In contrast, addition of ascorbic acid to KCL22/SR cells resulted in a decrease in Nrf2-DNA binding and decreases in levels of γ-GCSl mRNA and GSH. Consistent with these findings, ascorbic acid partly restored imatinib sensitivity to KCL22/SR.**

Conclusion. **Changes in the redox state caused by antioxidants such as ascorbic acid can overcome resistance to imatinib via inhibition of Nrf2-mediated gene expression.** © **2004 International Society for Experimental Hematology. Published by Elsevier Inc.**

Imatinib (imatinib mesylate: Novartis Pharmaceuticals, Basel, Switzerland), a specific BCR/ABL tyrosine kinase inhibitor, has been shown to be effective for treatment of chronic myelogenous leukemia (CML) in blast crisis (BC) and in chronic phase (CP) [1–2]. In recent clinical studies of imatinib with large numbers of BC patients, around 50% of patients achieved hematologic response [3]. However, drug resistance is a major problem for imatinib treatment of CML patients in BC because substantial numbers of patients have relapsed relatively soon after treatment with imatinib [2,3]. Previous studies have demonstrated possible mechanisms involved in resistance to imatinib. These include amplification of and mutations in the BCR/ABL gene, increased expression of BCR/ABL protein and p-glycoprotein, and an increase in serum α1 acid glycoprotein [4–9]. However, some imatinib-resistant cells show none of these changes [6], suggesting that the mechanisms involved in resistance to imatinib are very complex.

Nrf2, a member of the CNC family of basic region-leucine zipper transcription factors, has been shown to bind to antioxidant-responsive element (ARE) [10,11]. ARE has been found in the promoter region of several detoxifying and antioxidative stress genes such as γ-glutamylcystein synthetase (γ-GCS) and glutathione-S-transferase (GST). Nrf2 contains 6 conserved domains: Neh1 to Neh6. Previous analysis has shown that Keap1, a homologue of the Drosophila actin-binding protein Kelch, binds to the Neh2 domain of Nrf2

Offprint requests to: Tadashi Nagai, M.D., Ph.D., Jichi Medical School, 3311-1 Yakushiji, Minamikawachi-machi, Kawachi-gun, Tochigi 329-0498, Japan; E-mail: t-nagai@jichi.ac.jp

0301-472X/04 $–see front matter.
doi: 10.1016/j.exphem.2004.01.007

in cytoplasm in a "nonstimulated"condition [12]. Activation inducers for Nrf2 such as oxidative stress cause dissociation of these two factors, resulting in migration of Nrf2 into the nucleus. There, Nrf2 binds to ARE as a heterodimer with other transcription factors, such as small Maf family proteins, and regulates ARE-mediated gene expression. Because induction of phase II detoxifying enzymes is significantly reduced in Nrf2 knockout mice and induction of some antioxidative stress genes such as hemeoxygenase I is severely impaired in Nrf2-deficient macrophages [13,14], it is thought that Nrf2 is necessary for expression of antioxidative stress genes as well as phase II detoxifying enzymes.

γ-GCS, the rate-limiting enzyme of the glutathione (GSH) synthetic pathway, catalyzes condensation of L-glutamate and L-cystein, to form L-γ-glutamylcysteine [15]. GSH, a prominent cellular nonprotein thiol, functions as a cellular antioxidant, and is thus critical for maintenance of redox balance [16]. In addition to these functions, it has been shown that GSH has effects on MAP kinase signaling and activity of the transcription factor NF-κB [17–19]. Also, it is involved in detoxification of substances in cells, via conjugation and transportation of substances out of cells [20]. Previous studies show that GSH is involved in resistance to some anti-cancer drugs, including cisplatin, doxorubicin, cytosine arabinoside, and daunorubicin [21,22]. γ-GCS is a heterodimer of heavy and light subunits: the catalytic domain is in the heavy subunit; the light subunit is important for regulation of the enzyme activity. Analysis of structure and function of the γ-GCS gene has shown that several cis-elements, including AP-1 and NF-κB binding sites, may be important in expression of this gene, and indicates that ARE is critical for expression of this gene [23].

In the present study, we found that γ-GCSl mRNA levels, GSH concentration, and levels of Nrf2/DNA complex at the ARE of the γ-GCS light subunit (γ-GCSl) gene promoter were higher in the imatinib-resistant BCR/ABL$^+$ cell line KCL22/SR than in the imatinib-sensitive parental cell line KCL22. We also found that ascorbic acid (AA) suppressed migration of Nrf2 to the nucleus, resulting in inhibition of GSH synthesis and restoration of sensitivity to imatinib in KCL22/SR cells.

Materials and methods

Cell culture

KCL22 is a BCR/ABL$^+$ cell line that was established from peripheral blood cells of a patient with CML in BC [24]. KCL22/SR is an imatinib-resistant cell line that was derived from KCL22 in our laboratory [25]. Cells from these lines were grown in RPMI1640 medium supplemented with 10% fetal bovine serum and split every 3 to 4 days. KCL22/SR cells were maintained in the presence of 0.5 mM imatinib. To evaluate effects of GSH on sensitivity of KCL22 cells to imatinib, KCL22 cells were incubated in the presence of 10 mM glutathione monoestel [26] for 24 hours prior to addition of various concentrations of imatinib. An MTT [3-(4,5-dimethylthiazol-2-yl)-2,5-diphenyl tetrazolium bromide] assay was performed to evaluate cytotoxicity, and IC_{50} values were determined from dose-response curves. To examine effects of AA, KCL22/SR cells were cultured without imatinib for 3 days, and were then incubated with 0.5 mM imatinib or 0.125 mM AA for 72 hours. Viable cells were counted by trypan blue exclusion after various periods of incubation.

Determination of glutathione concentration

A total of 2×10^6 cells were harvested and used to assay for glutathione. Glutathione concentration was measured using the GSH-400 system (OXIS Int. Inc., Portland, OR, USA), essentially according to the manufacturer's protocol.

Determination of intracellular peroxides in KCL22/SR cells

Cells were incubated with 2′,7′-dichlorofluorescein diacetate (Molecular Probes, Eugene, OR, USA) as the fluorogenic substrate for 30 minutes. The level of intracellular peroxides was determined by flow cytometry, as described previously [27].

RNA blot analysis

Total RNA was isolated from KCL22 and KCL22/SR cells using the acid guanidium thiocyanate–phenol chloroform method [28]. Northern blot analysis was performed as described elsewhere [29]. Human cDNA clones of γ-GCS light and heavy subunits [21] were used as probes. The HG126 clone of the ribosomal RNA gene was used as an internal control.

Western blot analysis

Total cell lysate and nuclear extract were prepared from 1×10^7 cells, using a method described elsewhere [30]. Protein concentration was determined using a Protein Assay Kit (BioRad, Hercules, CA, USA). A 10% polyacrylamide gel was used to separate 10 μg of protein electrophoretically. Immunoblotting and detection by enhanced chemiluminescence were performed as described elsewhere [31]. Rabbit polyclonal anti-Nrf2 (C-20) antibody was purchased from Santa Cruz Biotechnology, Inc. (Santa Cruz, CA, USA). Mouse anti-glyceraldehyde-3-phosphate dehydrogenase monoclonal antibody, which was used as an internal control, was purchased from Chemicon International (Temecula, CA, USA).

DNA gel mobility shift assays

To evaluate the DNA binding activity of Nrf2, DNA gel mobility shift assays were performed using the oligomer 5′-CTACGATTTC-TGCTTAGTCATTGTCTTCC-3′, which contains the 11-bp ARE and its flanking sequences. This oligomer was end-labeled with [γ-^{32}P] ATP by T4 polynucleotide kinase (Boehringer Mannheim Corp., Indianapolis, IN, USA). The antisense oligomer was then added to the ^{32}P-end-labeled oligomer to yield a double-stranded probe. Nuclear extracts (5 μg) were incubated with the ^{32}P-labeled oligomer for 15 minutes on ice, in a reaction mixture containing 20 mM HEPES buffer (pH 7.8), 60 mM KCl, 0.2 mM EDTA, 6 mM $MgCl_2$, 0.5 mM dithiothreitol (DTT), 10% [v/v] glycerol and 1.5 μg of an equimolar mixture of poly (dI-dC) and poly (dA-dT). For competition assays, the AREm oligomer 5′-CTACGATTTCTGCTTCGTCCTTGTCTTCC-3′, which is a mutated ARE containing two transversions, was used in double-stranded form. In antibody-mediated competition assays, 3 μL of anti-Nrf1, anti-Nrf2, anti-c-Jun, and anti-GATA-2 antibodies (Santa Cruz Biotechnology, Inc., Santa Cruz, CA, USA) were first incubated with nuclear extracts on ice for 20 minutes and were then incubated with the probes for 10 minutes. This mixture was then

loaded onto a 4% polyacrylamide gel and electrophoresed at 150 V and 4°C.

Transfection and luciferase assays

We cotransfected 2 μg of luciferase reporter plasmid fused to human γ-GCSl promoter region (pGCSl-pro; contains ARE and AP-1 binding sites) and 1 μg of effector plasmid or pRL-CMV (internal control) into KCL22/SR cells using TransFast reagent (Promega Corp., Madison, WI, USA), according to the manufacturer's protocol. Briefly, a total of 1×10^6 cells were incubated with the plasmids and TransFast, in 1 mL of medium without serum for 1 hour. Then, 5 mL of fresh medium containing 10% serum was added, and incubation was continued for 48 hours. Luciferase activity was determined using the Dual-Luciferase Reporter Assay System (Promega). Effector plasmids expressing full-length (pcDNA3/mNrf2#0) and dominant-negative (pcDNA3/mNrf2#Eco del) mouse Nrf2 were kindly provided by Drs. K. Ito and M. Yamamoto (Tsukuba University, Tsukuba, Japan).

Results

Formation of Nrf2/DNA complex at ARE was increased in KCL22/SR cells

It has been reported that ARE binds with CNC family transcription factors and plays a critical role in expression of a number of antioxidant and detoxifying enzymes such as γ-GCS, which is a rate-limiting enzyme in GSH synthesis. To clarify whether ARE-mediated regulation of gene expression is involved in imatinib resistance, we first examined DNA binding activity at ARE in the human γ-GCSl gene promoter of KCL22 and KCL22/SR cells using a gel mobility shift assay. The band that was detected was much more prominent in KCL22/SR than in KCL22 (Fig. 1A). This band was completely suppressed by addition of anti-Nrf2 antibody, but not by anti-Nrf1, anti-c-Jun, or anti-GATA-2 antibodies, indicating that it is an Nrf2/DNA complex (Fig. 1B). The increase in Nrf2/DNA complex formation in KCL22/SR cells is not due to increased Nrf2 expression, because there was no difference in Nrf2 protein level between KCL22 and KCL22/SR cells when total cell lysate was used for immunoblot analysis (Fig. 1C). However, when nuclear extracts were used for immunoblot analysis, the level of Nrf2 protein was much higher in KCL22/SR cells than in KCL22 cells (Fig. 1C). These results suggest that induction of Nrf2/DNA complex formation in KCL22/SR cells is caused by movement of Nrf2 from cytoplasm to nucleus.

Nrf2 increased γ-GCS light subunit gene promoter activity

To clarify whether the Nrf2/DNA complex is active in transcription, we examined the effect of Nrf2 on ARE-mediated promoter activation by luciferase reporter assay. Results of these experiments are summarized in Figure 2. When pGCS-pro, which contains ARE and AP-1 sites, was transfected into KCL22/SR cells, luciferase activity increased 150-fold over control activity, which was obtained by transfection of pGL3-Basic promoterless construct. Cotransfection of

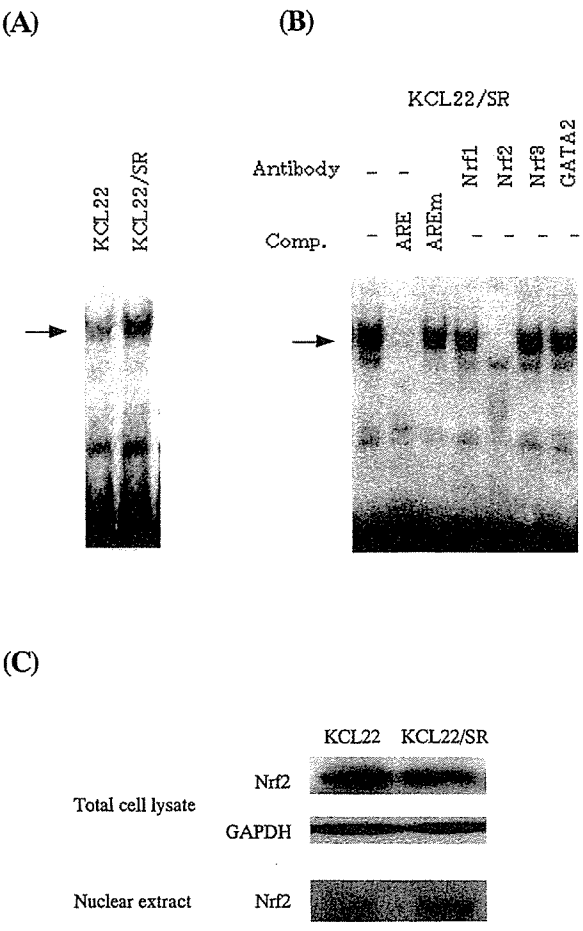

Figure 1. Formation of a DNA-protein complex at antioxidant responsive element (ARE) of the human γ-glutamylcystein synthetase light subunit (γ-GCSl) gene promoter. (**A**): Nuclear extracts (5-mg aliquots) from KCL22 or KCL22/SR cells were incubated with end-labeled oligomers corresponding to ARE. (**B**): Competition assays were performed with a 200-fold molar excess of the indicated oligonucleotides or anti-Nrf2, anti-Nrf1, anti-c-Jun, and anti-GATA-2 antibodies. (**C**): Total cell extracts or nuclear extracts were prepared, separated by SDS-polyacrylamide gel electrophoresis, transferred onto a membrane, and reacted with anti-Nrf2 antibody. The expression of glyceraldehyde-3-phosphate dehydrogenase (GAPDH) was examined as an internal control.

the Nrf2 expression vector pcDNA3/Nrf2#0 resulted in a significant increase in luciferase activity. In contrast, expression of the dominant-negative form of Nrf2, which lacks the transcriptional activation domain (pcDNA3/mNrf2#Eco del), suppressed luciferase activity (Fig. 2). These results suggest that ARE in the γ-GCSl gene promoter is active in transcription, and that induction of Nrf2/DNA complex formation at ARE leads to upregulation of promoter activity.

GSH level is higher in KCL22/SR than in KCL22 cells

The level of γ-GCSl mRNA was significantly higher in KCL22/SR cells than in KCL22 cells (Fig. 3A), and the concentration of GSH was 1.5-fold higher in KCL22/SR cells than in KCL22 cells (Fig. 3B). Because γ-GCS is a rate-limiting enzyme of GSH synthesis, upregulation of γ-GCSl

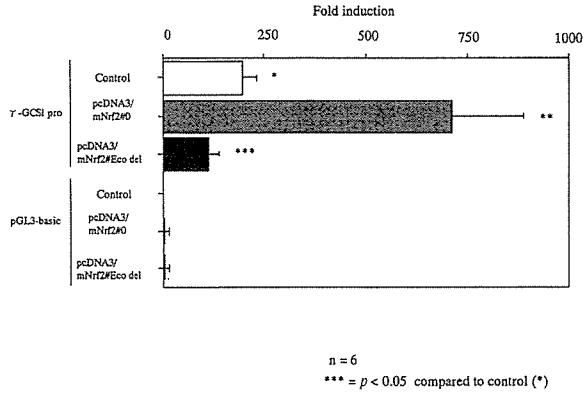

Figure 2. Effect of Nrf2 on the enhancer activity of the human γ-GCSl gene promoter. KCL22/SR cells were transfected with luciferase reporter pGCS-pro or pGL3-Basic together with 1 μg each of pcDNAmNrf2#0 or pcDNA3mNrf2#Eco del effector molecules. Firefly luciferase activity was normalized on the basis of Renilla luciferase activity. The results are expressed as the ratio of firefly luciferase activities of cells transfected with pGL3-basic without any effector molecule.

expression may lead to accumulation of GSH in KCL22/SR cells.

In previous studies, GSH was implicated in resistance to some anti-cancer drugs [9,10]. To clarify whether increased GSH levels are important for resistance to imatinib, we examined the effect of a GSH monoester on sensitivity to imatinib. Addition of a GSH monoester to imatinib-sensitive KCL22 cells resulted in a 2.8-fold increase in the IC_{50} value of imatinib (Fig. 3C). We also examined the effect of buthionine sulfoximine (BSO; a potent inhibitor of γ-GCS) on imatinib sensitivity of KCL22/SR cells, but failed to obtain usable results because of the severe toxicity of BSO.

Ascorbic acid reduced Nrf2/DNA complex formation by inhibiting movement of Nrf2 into nucleus

Because oxidative stress promotes movement of Nrf2 into the nucleus, it is likely that a shift in intracellular redox balance toward a reduced state inhibits movement of Nrf2 in KCL22/SR cells. To verify this hypothesis, we examined the effect of AA (a reducing reagent) on Nrf2/DNA complex formation. Peroxide levels in KCL22/SR cells were reduced by addition of 0.125 mM AA (Fig. 4A), strongly indicating that AA acts as an antioxidant. Formation of Nrf2/DNA complex in KCL22/SR cells was markedly decreased by addition of 0.125 mM AA (Fig. 4B) without any change in Nrf2 protein level in total cell lysate (Fig. 4C), suggesting that AA inhibited movement of Nrf2 into the nucleus.

Ascorbic acid restores imatinib sensitivity in KCL22/SR cells

We next examined the effects of AA on GSH synthesis and growth of KCL22/SR cells. Although the level of γ-GCS heavy subunit mRNA was not changed (data not shown), that of γ-GCSl mRNA was significantly reduced by addition of 0.125 mM AA (Fig. 5A). Simultaneously, GSH concentration in KCL22/SR cells was reduced (Fig. 5B), indicating that AA inhibited GSH synthesis. AA had no inhibitory effect on

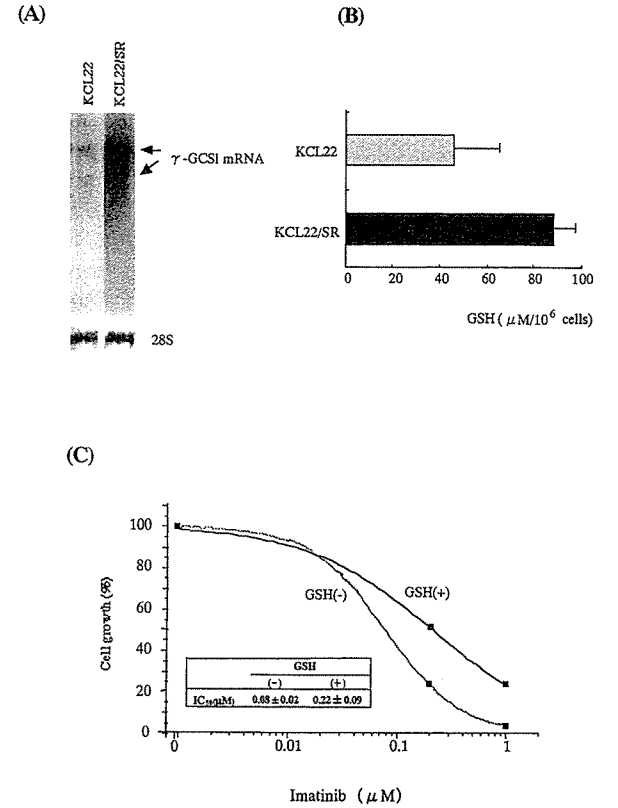

Figure 3. Glutathione synthesis in KCL22/SR cells. (**A**): The levels of γ-GCSl mRNA were analyzed by Northern blotting. The filter was rehybridized to a ribosomal RNA probe. 28S ribosomal RNA bands are shown. (**B**): Glutathione (GSH) concentration was measured with the GSH-400 system (OXIS Int. Inc.), using 2×10^6 KCL22 or KCL22/SR cells, as described in Materials and Methods. (**C**): KCL22 cells were cultured with various concentrations of imatinib for 72 hours in the presence or absence of GSH. The ratio of IC_{50} is shown in the figure.

growth of KCL22/SR cells when administered alone, but combined treatment of KCL22/SR cells with imatinib and AA resulted in inhibition of cell growth (Fig. 5C). Consistent with these findings, addition of 0.125 mM AA resulted in a 50% decrease in the IC_{50} value of imatinib for KCL22/SR cells, suggesting that AA at this concentration is not directly cytotoxic but restores sensitivity of KCL22/SR cells to imatinib via, at least in part, suppression of intracellular GSH level.

Formation of Nrf2/DNA complex is increased in another imatinib-resistant cell line

To clarify whether an increase in formation of Nrf2/DNA complex occurs in imatinib-resistant cells in general or occurs only in KCL22/SR cells, we performed gel mobility shift assays using nuclear extracts of the imatinib-resistant cell lines K562/SR and KU812/SR, which were recently cloned in our lab, and their imatinib-sensitive parental strains (K562 and KU812, respectively). As shown in Figure 6, while there was no difference in the level of Nrf2/DNA complex between KU812/SR and KU812, the level of Nrf2/DNA complex was higher in K562/SR than in K562. These

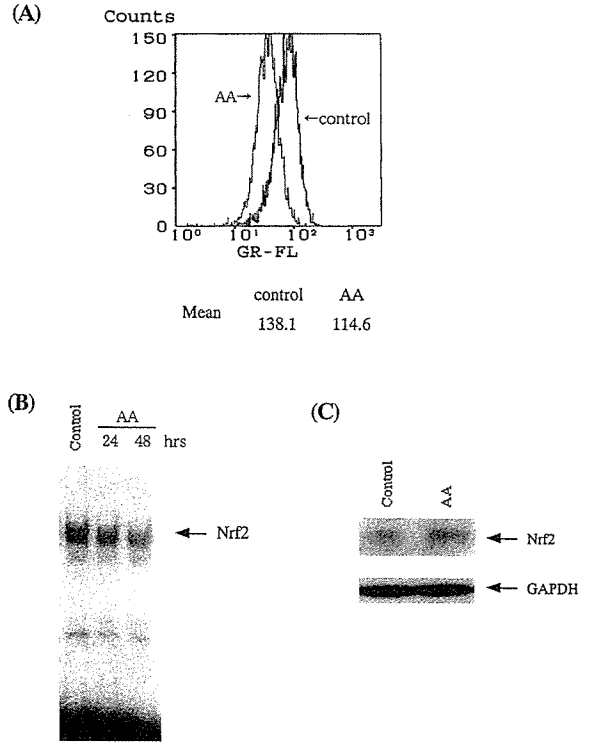

Figure 4. Effect of ascorbic acid on formation of Nrf2/DNA complex. (**A**): KCL22/SR cells were incubated with 0.125 mM ascorbic acid (AA) for 6 hours. The level of intracellular peroxides was determined by flow cytometry, as described in Materials and Methods. Decreased green fluorescence correlates with decreased peroxide levels. (**B**): KCL22/SR cells were incubated with 0.125 mM AA. The level of Nrf2/DNA complex formation at various time points was evaluated by gel mobility shift assay using oligomers corresponding to ARE. (**C**): KCL22/SR cells were cultured in the absence or presence of 0.125 mM AA for 24 hours. The levels of Nrf2 protein in total cell extracts were examined by immunoblot analysis using anti-Nrf2 antibody. The expression of glyceraldehyde-3-phosphate dehydrogenase (GAPDH) was examined as an internal control.

results suggest that induction of Nrf2 activity is involved in resistance to imatinib in some, but not all, imatinib-resistant cell lines.

Discussion

Recently, various new anti-cancer agents that target specific oncogenic molecules have been developed. Imatinib is one of the most successful of these reagents. However, a major problem with imatinib treatment is acquisition of resistance. In the present study, we used the imatinib-resistant BCR/ABL$^+$ cell line KCL22/SR to investigate the mechanisms of resistance to imatinb. KCL22/SR was cloned from the human BCR/ABL$^+$ cell line KCL/22. The IC_{50} value of imatinib for KCL22/SR is about 11.6-fold higher than that of KCL22, indicating that KCL22/SR has acquired significant resistance to imatinib [25]. Examination of KCL22/SR has revealed no mutations in the BCR/ABL gene and no increase in levels of BCR/ABL protein or P-glycoprotein. Given that the level of phosphorylated BCR/ABL protein is suppressed by imatinib treatment, these previous findings suggest that mechanisms independent of BCR/ABL activity are involved in the imatinib resistance of KCL22/SR [25]. The present results suggest that Nrf2 is involved in the imatinib resistance of KCL22/SR.

Nrf2 has been shown to regulate ARE-mediated gene expression. The present results demonstrate that formation of Nrf2/DNA complex at the ARE of the γ-GCSl gene promoter occurs at a significantly higher rate in KCL22/SR cells than in KCL22 cells (Fig. 1A). The amount of Nrf2/DNA complex was also increased in the imatinib-resistant cell line K562/SR, compared with its parental imatinib-sensitive line, K562 (Fig. 6), suggesting that this phenomenon occurs in many types of imatinib-resistant cells other than KCL22/SR cells. Consistent with these findings, the level of γ-GCSl mRNA was significantly higher in KCL22/SR cells than in KCL22 cells (Fig. 3A). The light subunit of the γ-GCS enzyme is a regulatory subunit and is important for regulation of γ-GCS activity. There was no difference in levels of γ-GCS heavy subunit (which contains a catalytic domain of γ-GCS) mRNA between KCL22/SR and KCL22 (data not shown). Nrf2-mediated induction of light subunit expression may result in upregulation of γ-GCS activity and a consequent increase in GSH synthesis (Fig. 3B). Addition of a GSH monoester to KCL22 cells resulted in an increase in the IC_{50} value of imatinib (Fig. 3C), suggesting that upregulation of GSH synthesis due to increased Nrf2 activity is involved, at least in part, in the imatinib resistance of KCL22/SR cells. Clarification of whether similar abnormalities are involved in the imatinib resistance in primary cells from imatinib-resistant leukemia patients is important, and such studies are now being carried out in our laboratory.

GSH has been shown to detoxify substances in cells via conjugation and transport out of the cell [20]. However, it is unlikely that GSH directly inactivates imatinib via conjunction in KCL22/SR cells, because imatinib still effectively suppressed BCR/ABL kinase activity in these cells. Thus, mechanisms of imatinib resistance due to GSH accumulation may involve effects on other biological functions, such as intracellular signaling. Since addition of GSH did not result in restoration of the imatinib-mediated reduction of phospho-ERK1/2 levels in KCL22 cells (data not shown), MAPK may not be involved in the mechanisms of imatinib resistance due to GSH accumulation.

The present findings strongly suggest that Nrf2 is a good molecular target for overcoming imatinib resistance. AA reduced peroxide levels (Fig. 4A) and suppressed levels of Nrf2/DNA complex at the ARE of the γ-GCSl gene promoter (Fig. 4B). Consistent with these results, treatment of KCL22/SR cells with AA resulted in reduced GSH level and enhanced sensitivity to imatinib (Fig. 5C). Although we have no clinical data on the effect of ascorbic acid in imatinib-resistant patients, an in vitro experiment showed that treatment with AA and imatinib also suppressed growth of leukemia cells from a patient with CML in BC who had relapsed during